2013

Setting behavior and shrinkage of high performance pavement concrete: Effect of supplementary cementitious materials, chemical admixtures and temperature

Qizhe Hou
Iowa State University

Setting behavior and shrinkage of high performance pavement concrete: Effect of supplementary cementitious materials, chemical admixtures and temperature

by

Qizhe Hou

A thesis submitted to the graduate faculty

in partial fulfillment of the requirements for the degree of

MASTER OF SCIENCE

Major: Civil Engineering (Civil Engineering Materials)

Program of Study Committee:
Kejin Wang, Major Professor
Vernon R Schaefer
Sri Sritharan

Iowa State University
Ames, Iowa
2013

DEDICATION

I would like to dedicate this thesis to my parents for their moral and financial supports. I would also like to delicate this thesis to my major professor Dr. Wang, Kejin without whose encourage I would not have been able to complete this achievement.

TABLE OF CONTENTS

ACKNOWLEDGEMENTS

Foremost, I would like to acknowledge my major professor Kejin Wang for her continuous support of my M.S. study. Her guidance always helped me during those two years, and I could not have imagined completing my M.S. without her.

I would like to thank my committee members, Vernon R Schaefer and Sri Sritharan, for their valuable time and efforts of serving my POS committee during their busy schedules. They were both made great efforts.

I also extend my thanks to Chengsheng Ouyang, who is my unofficial advisor for three years since I was an undergrad. His contributions on concrete setting behavior project were really significant. Moreover, I would like to thank to Chen Yu, who is a visiting scholar from China. I did learn a lot from her during the shrinkage project.

In addition, I would also like to thank teaching laboratory manager Donald Davidson, research laboratory manager Robert Steffes, for their kindly help and continuous support on my teaching/research assistant.

I want to say thank you to all my friends, officemates, the department faculty and staff for making my time at Iowa State University a wonderful experience.

The last but not the least, I would like to give very special thanks to my family for their love, encouragement and financial support.

ABSTRACT

The work presented in this thesis focuses on setting the behavior and shrinkage properties of high-performance pavement concrete and the effect factors, such as supplementary cementitious materials (SCMs), chemical admixtures, and temperature. The thesis consists of two papers: (1) the relation between setting behavior and the maturity of pavement concrete materials and (2) a simple statistical model to predict the shrinkage behavior of high-performance concrete containing supplementary cementitious materials.

In paper 1, setting behaviour and maturity of six different concrete mixtures under three different curing temperatures (18.3, 23.9, and 29.4°C, corresponding to 65, 75 and 85^{o}F) were investigated. The mixtures were made with two different retarders (ASTM Types B and D) and with 0 or 20% Class C fly ash replacement for Type I cement. The initial and final set times of these mixtures were measured by the penetration resistance method according to ASTM C 403. The temperature rise of the mixtures was monitored using a thermal couple, and the concrete maturity was then computed based on the time- temperature factor (TTF). A new approach is introduced for predicting concrete set time (penetration resistance) based on the concrete maturity (time-temperature factor). The results indicate that concrete penetration resistance well correlates with maturity measurements. This relationship enables engineers to assess setting behaviour of field concrete on site.

In paper 2, autogenous shrinkage and free drying shrinkage of nine different high performance concrete mixtures used for bridge decks and bridge overlays constructions were measured, and the total shrinkage (defined as autogenous shrinkage plus free drying shrinkage) was studied. The mixtures were systemically designed for evaluating effects of class C fly ash and ground granulated blast-furance slag replacement on shrinkage proporties. A simplified exponential model $\varepsilon_{auto/drying}(t)=a+b*e^{(c*t)}$ was introduced for describing and predicting shrinkage in high-performance concrete when different types and amounts of supplementary cementitious materials were used. This model fits for both autogenous and free drying shrinkage and is validated and proved by comparing measured value with predicted shrinkage value of an independent group of mixtures. The results indicate that compare to GGBF slag, fly ash performs much better to reduce the total shrinkage. Additionally, free drying shrinkage increases linearly with autogenous shrinkage between 0 and 14 days.

The results of the present study indicate that the concrete maturity method successfully describes the concrete setting behavior; and the exponential model successfully predicts the shrinkage behavior of high-performance concrete with SCMs. Additionally, the results indicate Class C fly ash replacement can reduce the total shrinkage and extend the setting time of high-performance concrete. The addition of Class C fly ash should be considered if extending concrete setting time and reducing the risk of shrinkage cracking are needed.

CHAPTER I. GENERAL INTRODUCTION

Introduction

In recent times, builders have commonly used high-performance concrete (HPC) in bridge decks and bridge overlays construction due to its high strength and rapid strength development. However, due to its properties—such as low water-to-cementitious material ratio, high doses of chemical admixtures, and high cementitious materials content—HPC always has a high potential risk of shrinkage cracking and exhibiting short setting time. At present, a study that evaluates and predicts shrinkage and setting behavior of high-performance concrete is necessary.

The purpose of this thesis is to use new approaches to describe the setting behavior and shrinkage properties of high-performance concrete. A comprehensive study was conducted to examine the effects of supplementary cementitious materials, such as fly ash, on the setting behavior and shrinkage of high-performance concrete.

For the setting behavior study (paper 1), six different HPC mixtures were designed to investigate how the 20% fly ash replacement, retarders, and curing temperatures would affect concrete initial and final setting times, as well as to investigate the relationship between the maturity index (a time–temperature factor) and penetration resistance under 18.3, 23.9, and 29.4°C. Theoretically speaking, for a specific mixture, if a concrete sample reaches an equal maturity index with another sample, its strength should also be equal. The results of this study indicate that concrete maturity is related to penetration resistance because penetration resistance relates to concrete strength. The penetration resistance -elapsed time curves at three different

temperatures should normalize as one curve if the datum temperature is properly selected. Once the normalized curve is established, the penetration resistance at a certain temperature can be predicted by measuring only the concrete maturity.

For shrinkage model study (paper 2), nine different HPC mixtures with different replacement rates of class-C fly ash and slag were systemically designed. Two of them were designed independently to use for a model validation test. Compared to normal-strength concrete, the amount of autogenous shrinkage of HPC is always considerable and contributes to the total shrinkage. Therefore, an exponential model was developed to add the autogenous shrinkage and free drying shrinkage together to determine the total shrinkage.

Those two studies both focused on high-performance pavement concrete with similar materials (such as fine aggregate, Class C fly ash) and mix proportions and, therefore, were highly related. In some cases, concrete setting behavior also affects shrinkage measurements. For instance, to measure the autogenous shrinkage of mortar in study 2, I first determined the corresponding final setting time according to the standard. For the 20% fly ash HPC mixture, rather that measuring its final setting, simply using the conclusion of the study 1, which meant simply multiplying the final setting time for the corresponding control mixture by a factor of 1.10.

Thesis Organization

This thesis is divided into four chapters. Chapter 1 gives an overall introduction and objectives of the thesis. Additionally, a brief literature review of concrete maturity, setting behavior, autogenous shrinkage, free drying shrinkage and shrinkage predicting modeling are conducted in this chapter.

Chapter 2 includes a selected paper titled “The relation between setting behavior and maturity of pavement concrete materials”, which is submitted to International Journal of Pavement Engineering.

Chapter 3 includes a selected paper titled “A Simple statistical model for prediction of shrinkage behavior of high performance concrete containing supplementary cementitious materials”, which is to be submitted to Journal of Construction and Building Materials.

Chapter 4 summarizes the major findings of the thesis and provides the recommendations for future research.

Literature Review

Concrete Maturity

Maturity method and function

The "maturity method" is used as a non-destructive approach to predict concrete strength by establishing the strength-maturity relationship. The maturity method according to ASTM C 1074-04 is defined as "a technique for estimating concrete strength that is based on the assumption that samples of a given concrete mixture attain equal strengths if they attain equal values of the maturity index."

There are two functions for calculation the maturity index: temperature-time factor (TTF) and equivalent age. In this thesis, the temperature-time factor is used to connect maturity with penetration resistance. The TTF function, or the Nurse-Saul function, is given below:

$$M(t) = \Sigma [(T_a - T_0)\, \Delta t]$$

Where M(t) is the TTF at age of t, Δt is a time interval, T_a is average concrete temperature during time interval Δt, and T_o is the datum temperature. (1)

The maturity function is depended based on the temperature sensitivity of the concrete strength development at early age. (2) Generally, maturity factor is affected by factors such as ambient temperature, relative humidity, and wind during construction process. Additionally, other factors such as cement type, pozzolans, SCM and water to cement ratio are also contributed to maturity factor. The application of maturity method is to predict strength in field by developing the maturity curve of given mixture in the laboratory. (3)

Datum Temperature

Datum temperature is defined as the temperature below which there is no strength development. (2) Datum temperature, or T_o at the TTF function above, may depend on the type of cementitious materials, type and dosage of chemical admixtures or other factors which can affect cement hydration rate. The ASCT C1074 recommends 0^oC for type I cement without admxitures and a curing temoerature ranges from 0 to 40 ^oC. (1) Table 1 presents the range and value of datum temperature that were determined based on the experimental work. However, the State DOTs always select -10^oC or 0^oC as the default datum temperatures to calculate concrete maturity. Table 2 below shows the datum temperature used by State DOTs. A datum temperature of $-10\ ^oC$ was selected by Iowa DOT, and which was also used in this study.

MnDOT office of materials did a series of concrete maturity test to predict the concrete strength in field. The maturity-strength curves at three different datum temperatures, 0^oC, -5^oC and -10^oC were established. It was found that a datum temperature of 0^oC is too high. The maturity-strength curves related better under datum temperatures of -5^oC and -10^oC. (3)

Table 1. Literature study of different datum temperature

Materials	Curing Temp.	T_0	References
Type I Cement without Admixture	0 to 40 ^{o}C	0 ^{o}C	Carino,1984 (4)
Type I Cement with Varied SCMs	8 ^{o}C, 23 ^{o}C, 40 ^{o}C	-1.3 to 3.4 ^{o}C	Brooks ,2007 (5)
Maryland DOT Pavement Concrete	4.4 ^{o}, 21.1 ^{o}, 32.2 ^{o} C	3.8 ^{o}C	R. Johnson,2011 (6)
AKDOT&PF Type I/II PC	-	-2.0 to 4.5 ^{o}C	Y. Dong, 2009 (7)
Type I/II cement with fly ash	50 ^{o}F & 90 ^{o}F	-2.66 to -7.17 ^{o}C	Wang K, 2003 (8)

Table 2. Datum temperature used by State DOTs

State DOTs	Specification	T_0 (^oC)
Alabama	ALDOT-425	0
Indiana	ITM 402-04T	-10
Iowa	IM 383	-10
Kansas	KT-44	-10
Kentucky	64-322-08	-10
Missouri	Section 507	-10
Ohio	Supplement 1098	0
Tennessee	Developing	-10
Texas	Tex-426-A	-10
Wisconsin	CMM 8.70	0

Concrete Setting Behavior

Penetration Resistance Test

Setting time of concrete can be obtained by testing a representative mortar sample sieved of the corresponding concrete, according to ASCT C403. The mortar is curried at the certain ambient temperature, and at regular time periods the measurement is taken by penetrating a standard needle 1 inch into the mortar. The initial and final setting time can be determined by plotting penetration resistance vs. elapsed time. Initial set and final set are defined as the times when the penetration resistance reaches to 500 psi [3.5 MPa] and 4000 psi [27.6 MPa], respectively. (9)

Temperature Affecting on Setting Time

Temperature affects concrete setting behavior due to it affecting hydration rate of cement. A clear linear relationship between concrete initial setting time and temperature was established as shown in figure 1 (a). Additionally, a linear relationship between

inverse of setting time and inverse of absolute temperature was also found. Conclusion can be made that the setting times for any temperature can be predicted based on the linear relationship by only measuring setting times at two extreme temperatures. The figure 1 (b) can be used to determine the activation energy referring to the method in ASTM C1074. (10)

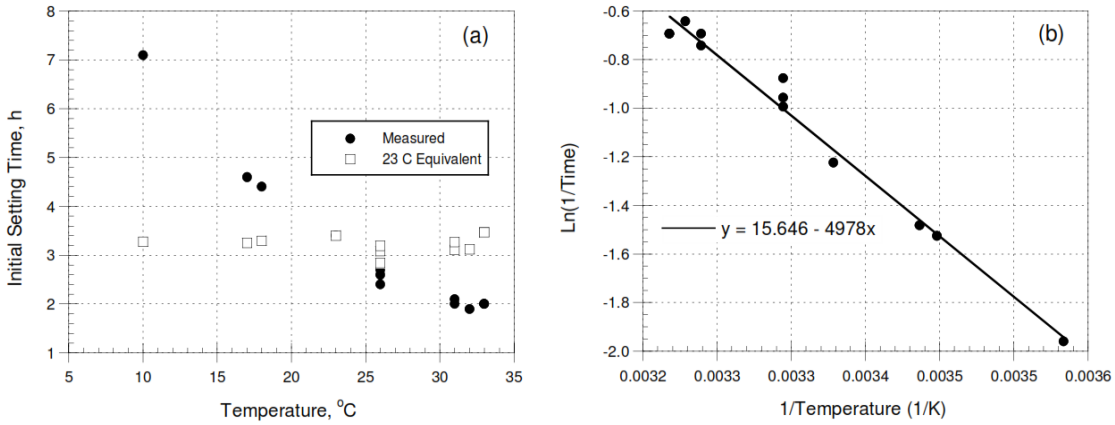

Figure 1. (a) Initial drtting time vs. temperature (b) inverse of setting time vs. inverse of absolute temperature *(Pinto,R.C 1999)*

Figure 2 (a) below shows a signicicant effect of temperature on concrete setting time. The temperature for hot, control and cold range from 32-41^{o}C, 20-24^{o}C and 4-13^{o}C respectively. The concrete strength development is much quicker at hot condition compared to the one at cold condition. Figure 2 (b) shows setting-maturity relationship by using equivalent age method. An activation engergy value of 26,700 J/mol was used to determine equivlent age. (11)

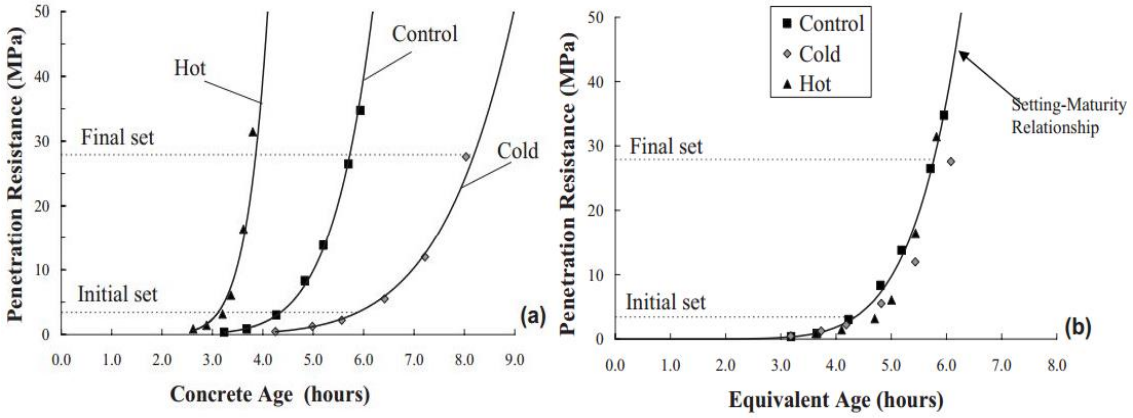

Figure 2. Results for the 30% slag mixture: (a) effect of temperature on setting time, (b) setting-maturity relationship *(Samuel A. Wade, 2010)*

SCMs Affecting on Setting Time

GGBF Slag: The effects of slag on concrete setting time depend on factors such as curing temperature, present replacement, and slag composition (Grade). Generally the slag replacement at a lower temperature increases the concrete setting time, especially for slag replacement higher than 40%. (12) The temperature is the key factor for slag to affect setting time. For temperature greater that 20^{o}C (68^{o}F), it shown that 30% and 50% slag replacements decrease the setting time of concrete. (13) However, another study shows that for slag replacements of 30, 50 and 70%, there is no delay on setting time at temperature above 35 ^{o}C (95^{o}F). (14) For Grade 120 GGBF slag, research shows that it has very tinny effect on concrete setting time, thus, slightly accelerate concrete setting rate. (11)

Class F Fly Ash: The effects of class C fly ash and class F fly ash on concrete setting time are not all the same, since class C fly ash has a better early strength

development. (15) Generally, class F fly ash increases the setting time of concrete due to its poor early strength development.

Class C Fly Ash: In this thesis, only class C fly ash was studied. For concrete with high percent fly ash replacement, the final setting time can be extended up to 6 hours. (16) Resent study also compared the effects of class C fly ash and class F fly ash on concrete setting time. Experimental results show that for a same replacement level, class C fly ash has more ability to extend concrete setting time. (11) However, research also shows that the effect on concrete setting time depends on the fly ash content. The initial and final setting times were delay below 60% replacement, and beyond this replacement level the rapid setting occurred. (17)

Autogenous Shrinkage

Definition and Mechanism

Autogenous shrinkage of cement paste and concrete is defined as the macroscopic volume change occurring without moisture transferred to the exterior surrounding environment (18). According to physical analyses, the driving force of autogenous shrinkage of concrete is the change in the capillary pressure induced by self-desiccation in its cement matrix. Self-desiccation is caused by the balance between the absolute volume reduction (chemical shrinkage) and the building up of the capillary network. It seemed that the creation of the early hydrated products resulted in an autogenous swelling phenomenon that decreases with time. (19)

Measurement

Measurements of autogenous strain of cement paste have been carried out in two different ways: measurement of volumetric strain and linear strain. Volumetric measurement is performed by placing the fresh cement paste in a rubber membrane submerged in water. The change in volume of the cement paste is measured by the amount of water displaced. Linear measurement is performed by placing the cement paste in a rigid mould with low friction. The length change of the cement paste may be recorded at the end of the specimen. (20) In this thesis the linear strain measurement was conducted.

SCMs Affecting Autogenous Shrinkage

GGBF Slag: A research for high performance concrete was investigated the effects of water to cementitious material ratio, silica fume and GGBF slag on autogenous shrinkage. The results indicated GGBF Slag increases autogenous shrinkage increment at later ages. (21) Another research conducted the autogenous shrinkage based on a series of mixtures with GGBFS replacement level of 0%, 30%, and 50% at different w/c. The result shows higher the slag replacement level, the greater the autogenous shrinkage at the same w/cm. (22)

Fly Ash: Test results (23) showed that autogenous shrinkage increased corresponding to the increase in the degree of hydration of fly ash. Moreover, it was found that the total quantity of Al_2O_3 in cement–fly ash samples affected autogenous shrinkage at early ages, but the long-term influence was very small. The autogenous

shrinkage and the pore structure of the hardened cement paste with the combination of fly ash and silica fume, or fly ash and blast furnace slag were tested (24). The results indicated that fly ash can reduce the autogenous shrinkage, and silica fume can increase the autogenous shrinkage, and the effect of blast furnace slag is between the two above.

Free Drying Shrinkage

Definition and Mechanism

The free drying shrinkage is defined as the shrinkage occurring in a specimen that is allowed to dry, according to ACI. (25) As shown in Figure 3, there are two cement particles at the surface of a paste subjected to drying. The evaporating water (W) exceeds the bleed water moving to the surface from within the concrete, which can generate stress and causes the meniscus to be lowered with the increasing the capillary pressure. (26)

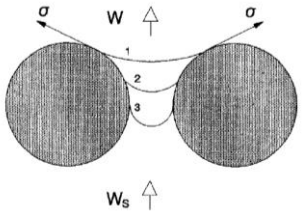

Figure 3. Stresses pulling the water meniscus lower between two cement particles due to moisture transfer and capillary pressure development, (*Radocea (1992)*

The drying mechanisms causing shrinkage are dependent on the internal pore spaces. Figure 4 described the various pore sizes along with the solid particles of the hydrated cement paste. The interaction of the pore spaces and internal water is influenced by the surrounding environment. During drying process of fresh concrete, the evaporation rate exceeds the amount of bleed water. The free surface that extra water is lost will move into the concrete body as evaporation continues. The loss of internal water causes the drying shrinkage. (27)

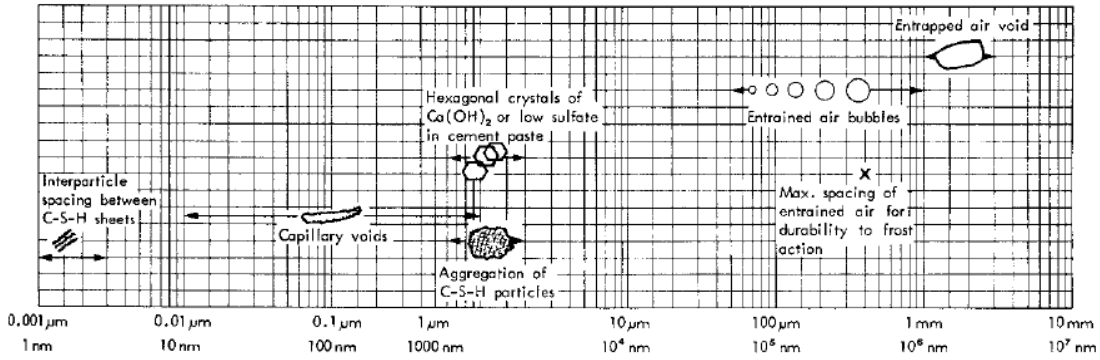

Figure 4. Distribution of soils and pores in hydrated cement paste, (*Mehta and Monteiro 1993)*

SCMs Affecting Free Drying Shrinkage

GGBF Slag: Study shows that the certain percent slag replacement will reduce the free drying shrinkage of concrete. Due to the pozzolanic reactions of the slag replacement in the cement matrix, the concrete pore structure becomes stronger, therefore resistance to shrinkage deformation. (28)

Fly Ash: The fly ash replacement generally reduces concrete free drying shrinkage. It was found that the replacement levels of 20% and 40% decreased free drying shrinkage of 16% and 40% respectively. (29) Fly ash behaves as a shrinkage reducer for cement paste due to reduce the water requirement. (30)

Existing Concrete Shrinkage Models

JSCE Specification 2002

"JSCE model" was first developed by the Japanese Society for Civil Engineers in 2002 and constituted a major modification for the 1996 model. Different from the most of models, JSCE Specification 2002 is the one that takes autogenous shrinkage into consideration. In this study, shrinkage for high strength (high performance) concrete and conventional concrete were considered separately and differently. Figure 5 below shows the shrinkage composition in conventional concrete 5(a) and high strength concrete 5(b). As shown below the autogenous to total shrinkage ratio in high strength concrete is much greater than conventional concrete, which indicates the autogenous shrinkage in high strength concrete cannot be negligible. Therefore the total shrinkage in high strength concrete was defined and modeled as the sum of both autogenous and free drying shrinkage.

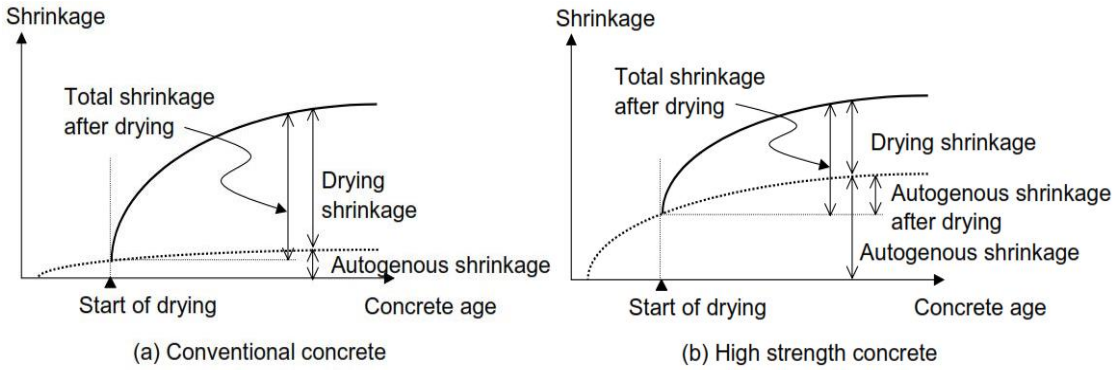

Figure 5. Shrinkage in conventional and high-strength concrete (Kenji Sakata, 2004)

As mentioned, the autogenous shrinkage and free drying shrinkage of high strength concrete were predicted separately, as equations shown below:

$$\varepsilon'_{cs}(t,t_0) = \varepsilon'_{ds}(t,t_0) + \varepsilon'_{as}(t,t_0)$$

$$\varepsilon'_{ds}(t,t_0) = \frac{\varepsilon'_{ds\infty} \cdot (t-t_o)}{\beta + (t-t_o)}$$

$$\varepsilon'_{as}(t) = \gamma \varepsilon'_{as\infty}\left[1 - \exp\left\{-a\left(t-t_s\right)b\right\}\right]$$

In the JSCE model, the major parameters considered are the water content, specimen volume to surface ratio, relative humidity, type of concrete and concrete 28 days compressive strength. The accuracy of model was tested and accepted based on different shrinkage database in Japan. (31)

ACI-209R-92

The model "ACI-209R-92" was first developed by Branson and Christiason in 1971, and then modified by ACI committee 209 in 1992. The general form of this classic

shrinkage model is shown below as a hyperbolic function of time multiplied by a set of correction factors such as relative humidity, curing method, sample size, type of cement, etc.

$$\varepsilon_s(t, t_0) = \varepsilon_{shu} . F_t . F_H . F_{th} . F_s . F_f . F_a . F_c$$

This model was empirically based only, which means it cannot model the phenomena of shrinkage. "ACI-209R-92" is one of the basic level and simple to use models since it only requires age of specimen, curing method, relative humidity, average thickness of specimen and cement type. However, the disadvantage of this model is the lack of accuracy. Figure 6 below shows the predicted shrinkage always higher than measured shrinkage at a low shrinkage value level. (32)

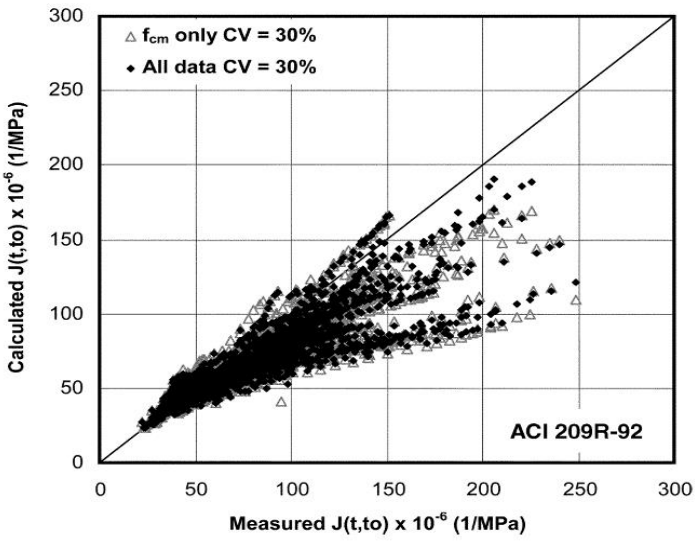

Figure 6. Calculated vs. measured for ACI 209R-92 ***(Gardner 2004)***

B3 Model

"B3 model" was a model following the development of BP Model and BP-KX Model at the Northwestern University (33), and the latest version was developed based on complex equations of more than 10 correction factors affecting shrinkage. Generally speaking, compare to the previous versions, the latest version is relatively simpler and fits better with the measured shrinkage. The latest version of B3 model considering correction factors such as specimen age, aggregate and cement content, cement type, 28 days compressive strength, curing method, relative humidity, shape of specimen, volume to surface ratio and water to cement ratio. (32) Because of the complexity of this model, some model parameters are always not available in the real application, such as compressive strength at 28 days. The model general form is given as follows:

$$\varepsilon_{sh}(t, t_0) = \alpha_1 . \alpha_2 \left[\frac{1.9}{100} w^{2.1} f_c^{-0.28} + 270\right] \frac{\left(\frac{607}{520}\right)^{1/2}}{\left(\frac{t_0 + \tau_{sh}}{4 + 0.85\,(t_0 + \tau_{sh})}\right)^{1/2}} (1 - h^3) \tanh \sqrt{\frac{t - t_o}{0.085\, t_0^{-0.08} f_c^{-1/4} . (k_s . 2 . v/s)^2}} . 10^{-6}$$

As mentioned above the limitation of this model is mostly due to its complex mathematical calculation. Additionally, this model is only applicable at the following situation:

1) $0.35 \leq w/c \leq 0.85$
2) $2.5 \leq a/c \leq 13.5$
3) $17\ \text{MPa} \leq \bar{f_c} \leq 70\ \text{MPa}$
4) $160\ \text{kg/m}^3 \leq c \leq 720\ \text{kg/m}^3$

GL2000

"GL 2000 model" is a modified version of GZ model that was developed by Gardner and Zhao (1993). (34) This model requires the parameters such as concrete age, 28 days concrete compressive strength, relative humidity, volume to surface ratio, and type of cement to evaluate the shrinkage strain. The model general form is shown as below:

$$\varepsilon_s(t) = \frac{1000}{10^6} \cdot k \cdot \left[\frac{30}{f_{cm28}}\right]^{\frac{1}{2}} \cdot [1 - 1.18\, h^4] \cdot \beta(t) \left(\frac{t - t_c}{t - t_c + 0.12 \left(\frac{V}{S}\right)^2}\right)^{\frac{1}{2}}$$

The limitation of this model is the complex mathematical calculations and low accuracy in comparison with other models. Additionally, the model is not valid when the relative humitity equals to 100%.

Reference

1. ASTM C 1074, 2004, "Practice for Estimating Concrete Strength by the Maturity Method," 2004 ASTM Standards Vol. 04.02, ASTM, West Conshohocken, PA

2. Nicholas J. Carino and H.S. Lew, 2001, The Maturity Method: From Theory to Application, American Society of Civil Engineers, Reston, Virginia, Peter C. Chang, Editor, 2001, 19 p.

3. Ryan J. R., Bernard I. I., Final Report of Demonstration of Concrete Maturity Test Process on the TH-694/TH-35E Interchange-Unweave the Weave, Minnesota Department of Transportation Office of Material and Road Research, MN/RC 2009-26

4. Carino, N. J., "The Maturity Method, Theory and Application", ASTM Journal of Cement, Concrete and Aggregates, Vol. 6, No. 2, Winter 1984, pp. 61-73.

5. Brooks, G. A., Schindler, K. A., and Barnes, W. R., "Maturity Method Evaluated for Various Cementitious Materials", Journal of Materials in Civil Engineering, December 2007

6. Johnson, R. and Hosten M. A., "Implementation of the Concrete Maturity Meter for Maryland", Final Report, Morgan State University, November 2011

7. Dong, Y., Song, R. and Dhungana, J., "Study of Concrete Maturity in Very Cold Weather", Final Report, Institute of Northern Engineering, University of Alaska, Fairbanks, December 2009

8. Wang, K. and Ge, Z., "Evaluating Properties of Blended Cements for Concrete Pavements", Ceneter for Portland Cement Concrete Pavement Technology, Iowa State University, Final Report, December 2003.

9. ASTM C 403, "Standard Test Method for Time of Setting of Concrete Mixtures by Penetration Resistance", the American Society of Testing and Materials, May 2008.

10. Pinto, R. C. A. and Hover, K. C., 1999, "Application of Maturity Approach to Setting Times", ACI Materials Journal, Vol. 96, No. 6, pp. 686-691.

11. Samuel A. W., Jeffery M. N., Anton K. S. and Robert W. B., Effect of Temperature on the Setting Behavior of Concrete, Journal of Materials in Civil Engineering, Vol. 22, No. 3, March 1, 2010
12. Brooks, J.J., Megat Johari, M.A., and Mazloom, M., "Effect of admixtures on the setting times of high-strength concrete," Cement and Concrete Composites, Vol. 22, 2000, pp. 293-301.

13. Eren, O., Brooks, J.J., and Celik, T., "Setting times of fly ash and slag-cement concretes as affected by curing temperature," Cement, Concrete, and Aggregates, Vol. 17, No. 1, 1995, pp.11-17.

14. Alshamsi, A.M., "Stiffening rates of blended-cement pastes in hot climates," Advances in Cement Research, Vol. 13, No. 1, 2001, pp. 11-16.

15. Gebler, S.H., and Klieger, P., "Effect of fly ash on physical properties of concrete," Fly Ash, Silica Fume, Slag, and Natural Pozzolans in Concrete Vol. 1, ACI, Detroit, 1986, pp.1-50.

16. Majko, R.M., and Pistilli, M.F., "Optimizing the amount of class C fly ash in concrete mixtures," Cement, Concrete, and Aggregates, Vol. 6, No. 2, 1984, pp. 105-119.

17. Naik, T.R., and Singh, S.S., “Influence of fly ash on setting and hardening characteristics of concrete systems,”ACI Materials Journal, Vol. 94, No. 5, 1997, pp. 355-360.

18. Ahmed Loukili, Abdelhafid Khelidj and Pierre Richard (1999), “Hydration kinetics, change of relative humidity, and autogenous shrinkage of ultra-high-strength concrete”, Cement and Concrete Research, Vol.29, 577-584.

19. Laurent Barcelo, Micheline Moranville and Bernard Clavaud (2005), “Autogenous shrinkage of concrete: a balance between autogenous swelling and self-desiccation”, Cement and Concrete Research,Vol.35, 177-183.

20. ASTM C1698-09. Standard Test method for autogenous strain of cement paste and mortar. In: ASTM international, West Conshohocken (PA); 2010.

21. Zhengwu Jiang, Zhenping Sun and Peiming Wang (2005), “Autogenous relative humidity change and autogenous shrinkage of high-performance cement pastes”, Cement and Concrete Research, Vol.35, 1539-1545.

22. K.M. Lee, H.K. Lee, et al (2006), “Autogenous shrinkage of concrete containing granulated blast-furnace slag”, Cement and Concrete Research, Vol.3, 1279-1285.

23. Pipat Termkhajornkit, Toyoharu Nawa, et al.(2005), “Effect of fly ash on autogenous shrinkage”, Cement and Concrete Research, Vol.35, 473-482.
24. Yue Li, Junling Bao and Yilin Guo (2010), “The relationship between autogenous shrinkage and pore structure of cement paste with mineral admixtures”, Construction and Building Materials, Vol.24, 1855-1860.

25. ACI 209-92, "Prediction of Creep, Shrinkage, and Temperature Effects in Concrete Structures,” Committee 209, American Concrete Institute, Michigan, 2008.

26. Radocea A.,A study on the Mechanisms of Plastic Shrinkage of Cement-Based Materials, PhD Thesis, CTH Goteborg, Sweden, 1992.

27. Koenders, E.A.B (1997). Simulation of Volume Changes in Hardened Cement-Based Materials, Ph.D. dissertation, Delft University Press, 171.

28. Li J., and Yao Y., “A study on creep and drying shrinkage of high performance concrete,” Cement and Concrete Research, 31(8), 1203-1206, 2001

29. Sounthararajan V. M. and Sivakumar A., Drying Shrinkage Properties of Accelerated Fly Ash Cement Concrete Reinforced with Hooked Steel Fiber, ARPN Journal of Engineering and Applied Sciences, Vol. 8, No. 1, January 2013

30. Tangtermsirikul, S., “Class C Fly Ash as a Shrinkage Reducer for Cement Paste,” ASTM Special Publication, American Society for Testing and Materials, Volume 153, 1995.

31. Sakata K., and Shimomura T., Recent Progress on and Code Evaluation of Concrete Creep and Shrinkage in Japan, Journal of Advanced Concrete Technology, 2(2), 113-140, 2004.

32. ACI 209.2R-08, “Guide for Modeling and Calculating Shrinkage and Creep in Hardened Concrete”, ACI Committee 209, American Concrete Institute, May 2008

33. Bazant and Baweja, Creep and Shrinkage Prediction Model for Analysis and Design of Concrete Structures: Model B3, American Concrete Institute Special Publication, 194(SP), 1-84, 2000

34. 34Gardner, N. J., and Lockman, M. J., 2001, “Design Provisions for Drying Shrinkage and Creep of Normal Strength Concrete,” ACI Materials Journal, V. 98, No. 2, Mar.-Apr., pp. 159-167

CHAPTER 2. THE RELATION BETWEEN SETTING BEHAVIOR AND MATURITY OF PAVEMENT CONCRETE MATERIALS

Modified from a paper submitted to International Journal of Pavement Engineering

Qizhe Hou, Chengsheng Ouyang and Kejin Wang

Abstract

In this study, setting behaviour and maturity of six different concrete mixtures under three different curing temperatures (18.3, 23.9, and 29.4°C) were investigated. The mixtures were made with two different retarders (ASTM Types B and D) and with 0 or 20% Class C fly ash replacement for Type I cement. The initial and final set times of these mixtures were measured by the penetration resistance method according to ASTM C 403. The temperature rise of the mixtures was monitored using a thermal couple, and the concrete maturity was then computed based on the time- temperature factor (TTF). A new approach is proposed for predicting concrete set time (penetration resistance) based on the concrete maturity (TTF). The results indicate that concrete penetration resistance well correlates with maturity measurements. This relationship enables engineers to assess setting behaviour of field concrete on site.

Keywords: fly ash; retarder; setting time; penetration resistance; maturity.

Introduction

Concrete setting behavior is important to construction operations, such as placing, surfacing, jointing, and formwork removal. A short initial set time may not provide engineers with sufficient time to work with concrete, while a prolonged final set time may cause raveling during jointing and may delay formwork removal.

ASTM C 403, Standard Test Method for Time of Setting of Concrete Mixtures by Penetration Resistance, has been widely used to determine set times of concrete mixtures. The elapsed times corresponding to 3.45 MPa (500 psi) and 27.58 MPa (4,000 psi) of the penetration resistance are specified as the initial and final set times of a concrete mixture, respectively. In order to ensure that concrete has certain workability for placement in field, Jones (1) proposed to use the elapsed time when a freshly mixed concrete mixture reaches 1.38 MPa (200 psi) of the penetration resistance as the working time limit, at which cementitious particles that suspend in a concrete system begin to contact each other, and the concrete mixture becomes less workable. The working time limit has been widely used by many states of the Department of Transportation.

Since concrete penetration resistance is greatly related to cement hydration process, which is in turn influenced by concrete curing conditions, the ASTM C 403 test method is often conducted at a given temperature. As a result, a set of penetration resistance curves of concrete under different curing temperatures is often developed so as to enable to assess the setting or working time of field concrete exposed to various environmental conditions. The development of such penetration resistance curves is both time consuming and labor intense.

In the present study, a new approach is developed to relate concrete penetration resistance to its maturity, namely time-temperature factor (TTF). Once established, this relationship can be used to predict the penetration resistance, setting or working time of field concrete using maturity measurements.

Objective

This study is aimed at developing a new approach to describe the relationship between penetration resistance and elapsed time of concrete based on the maturity concept.

Materials and Mix Proportions

Type I Portland cement and Class C fly ash were used, and their properties are listed in Table 1.

Crushed limestone, with nominal maximum size of 25.4 mm (1.0 inch), specific gravity of 2.67, and absorption of 1.14, was used as coarse aggregate. The gradation of the aggregate met the ASTM C 33 Size No. 57 requirements. River sand, with specific gravity of 2.64, absorption of 1.07, and fineness modulus of 3.08, was used as fine aggregate.

Table 1. Properties of type I cement and class C fly ash used

Compound (%)	CaO	Al_2O_3	SiO_2	Fe_2O_3	SO_3	K_2O	Na_2O	MgO	LOI	Specific Gravity	Fineness (m^2/kg)
Type I	63.5	5.45	19.8	2.56	3.12	0.71	0.02	3.07	2.65	3.14	408
Fly Ash - C	30.1	17.7	29.2	5.48	3.41	0.31	2.16	7.65	0.40	2.65	-

An air-entraining agent (AEA) and two commonly used retarding admixtures are used in the present study. The AEA used conforms to ASTM C 260. The two retarding admixtures, designated as Retarders 1 and 2, meet ASTM C 494 requirements for Type B (retarding) and Type D (water-reducing and retarding), respectively. Properties of these three non-chloride chemical admixtures are given in Table 2.

Table 2. Chemical and physical properties of two retarders and AEA used

	Retarder 1	Retarder 2	AEA
Chemical Characterization	Lignosulphonate solution with less than 1% of sodium hydroxide and gluceraldehyde	Sodium salt of organic acid mixture	Synthetic organic chemical with 5-10% of sodium olefin sulfonate, and 0.1-1.0% of glutaraldehyde
Specific Gravity	1.25	1.18	1.015
pH	7.8	10	10.0

The concrete mix proportion used is listed in Table 3. The cementitious materials are either pure Type I cement or the cement with 20% Class C fly ash replacement. The water-to-cementitious materials ratio is 0.41.

Table 3. Weight of material per cubic meter of concrete

Limestone	Sand	Cementitious*	Water	AEA	Retarder 1	Retarder 2
1,006 kg	822 kg	340 kg	139 kg	177 ml	1,105 ml	884 ml

* cement with and without 20% Class C fly ash replacement

The fresh concrete has slump in the range of 3 to 5 cm and air content approximate 6%. The strength of the hardened concrete is listed in Table 4.

Table 4. Compressive strength of concrete tested

Concrete Mixtures	Compressive Strength (MPa)		
	1 Day	7 Day	28 Day
No Retarder	15.3	31.8	46.1
No Retarder with FA	12.9	29.9	45.1
Retarder 1	9.5	28.8	41.5
Retarder 1 with FA	4.6	26.4	45.9
Retarder 2	8.0	34.3	46.7
Retarder 2 with FA	7.2	32.8	39.4

Sample Preparation and Penetration Test

Before mixing, all materials and tools were preheated to the prescribed temperature of 18.3^{o}C, 23.9^{o}C or 29.4^{o}C. After properly mixed according to ASTM C 192, concrete was sieved by a No. 4 sieve to obtain mortar. The mortar was then cast in a 150 x 200 mm cylinder container. The cylinder container was first filled with approximate 50 mm of concrete at bottom, followed by 140 mm of the sieved mortar at

top. The mortar was consolidated on a vibration table, and the surface bleeding water was absorbed by a dry rag. A temperature sensor was then inserted into the mortar approximately 75 mm below the surface, to monitor the change of concrete temperature.

Right after the casting, the mortar specimens were divided into three groups and cured at three different temperature conditions (65^{o}F/18.3^{o}C, 75^{o}F/23.9^{o}C and 85^{o}F/29.4^{o}C). These temperature conditions were achieved by using a water tank (18.3 and 29.4 ^{o}C) and an environmental chamber (23.9^{o}C), respectively. The environmental chamber was used to simulate a curing temperature of 23.9^{o}C because of lack of water tank. Figure 1 shows the typical temperature curves of tested specimens under the three curing temperatures. It is noted that the sample cured in the environmental chamber had a temperature rise after the target temperature of 23.9^{o}C was achieved at the elapsed time of 300 min. This is probably due to heat of cement hydration. Different from the water tank, the environmental chamber has little ability to help the timely dissipation of the heat in concrete to the environment.

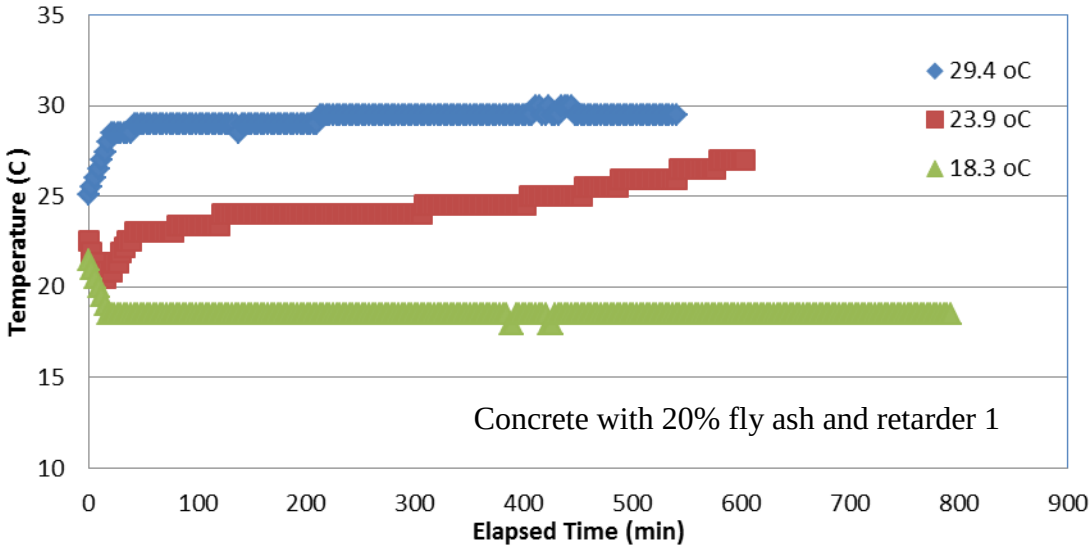

Figure 1. Typical temperature measurement

Figure 2. Device for penetration test

The penetration tests were performed for the mortar specimens according to ASTM 403. The test device is shown in Figure 2. There were six different sizes of needles with surface areas of 645, 323, 161, 65, 35, 16 mm^2 (1, 1/2, ¼, 1/10, 1/20, and 1/40 $in.^2$), respectively. The specimens were taken out from their curing environments

and tested at a room temperature. During the test, a needle of appropriate size, depending upon the degree of setting of the mortar, was inserted about 25 mm (1 in.) into the mortar. The applied pressure on the needle and the elapsed time were recorded. The time at which initial contact was made between cement and mixing water was defined as the zero elapsed time in this study. A typical relationship between penetration resistance and elapsed time obtained is illustrated in Figure 3.

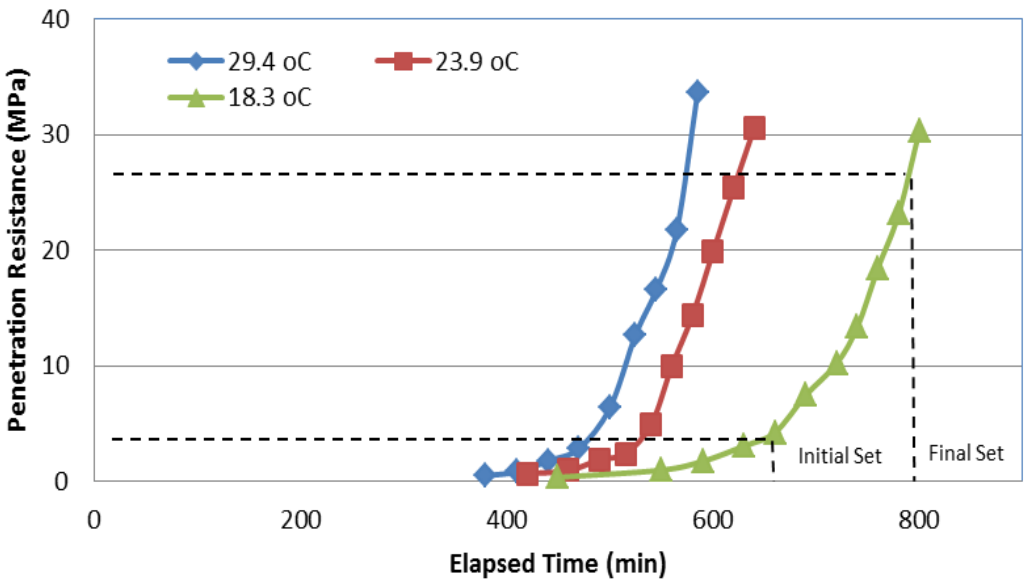

(a) With Retarder 1

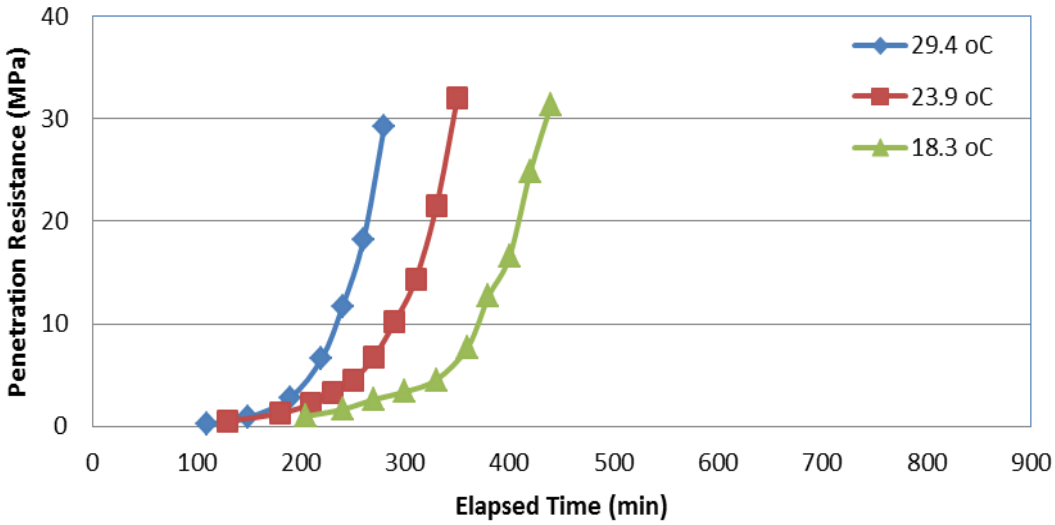

(b) Without Retarder

Figure 3. Typical penetration resistance vs. elapsed time (20% Fly Ash)

According to ASTM C 403, the elapsed times at 3.45 MPa (500 psi) and 27.58 MPa (4,000 psi) of the penetration resistance were generally regarded as the initial set time and final set time of mortar, respectively.

Results and Discussions

Summary of Concrete Set Time Results

Table 5 summarizes the initial set time and final set time for all six concrete mixtures at three different temperatures tested in this study.

Table 5. Concrete set times measured under different curing temperatures

Concrete Mixtures	Temperature (^{o}C)	Initial Set Time (min.)	Final Set Time (min.)
Retarder 1, 20% Fly Ash	29.4	480	575
	23.9	530	630
	18.3	645	792
Retarder 1, No Fly Ash	29.4	455	548
	23.9	480	580
	18.3	555	695
Retarder 2, 20% Fly Ash	29.4	278	370
	23.9	435	490
	18.3	575	680
Retarder 2, No Fly Ash	29.4	250	335
	23.9	360	480
	18.3	530	635
No Retarder, 20% Fly Ash	29.4	195	275
	23.9	230	342
	18.3	300	428
No Retarder, No Fly Ash	29.4	165	245
	23.9	195	290
	18.3	240	375

Effect of Curing Temperature

To better study the effect of temperature, the obtained initial/final set time values (Columns 3 and 4 in Table 5) were averaged and plotted against temperature in Figure 4. As expected, the initial/final set time decreased linearly with the increased curing temperature. From data regression, the following relationships between the initial/final set time (IS/FS) and temperature (T) was obtained:

$$IS\ (min) = -15.4(T) + 750 \qquad (R^2 = 0.99) \qquad (1)$$

$$FS\ (min) = -18.9(T) + 938 \qquad (R^2 = 0.98) \qquad (2)$$

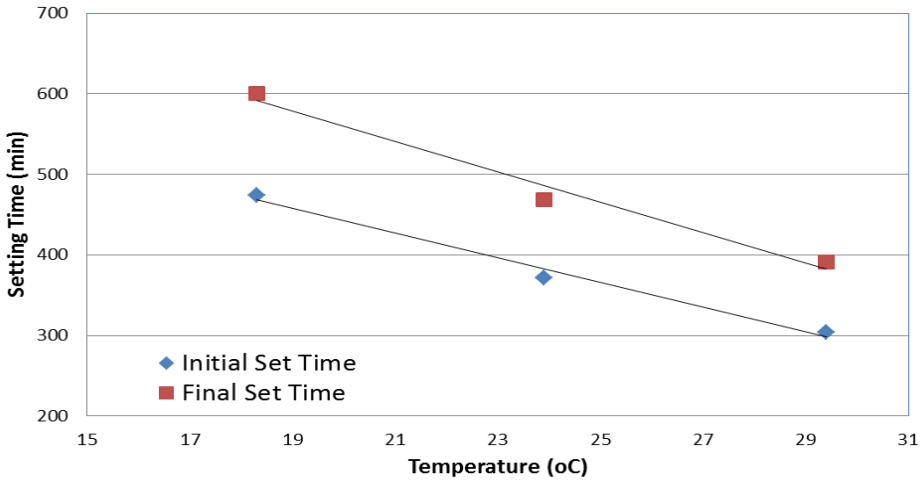

Figure 4. Effect of temperature on concrete set time

According to the linear relationship illustrated above, if curing temperature raises 1^{o}C, the initial set time and final set time will drop about 15 min and 19 min respectively. This relationship can be used in the field to adjust the estimated concrete set time if the curing temperature has been changed.

Effect of Retarders

Figure 5 illustrates the effects of the two retarders used in the study on concrete initial and final set times. As anticipated, both the retarders extended concrete set time. However, the degree of extension was higher for the concrete mixtures with 325 ml/100 kg of Retarder 1 than the mixtures with 260 ml/100 kg of Retarder 2. It is also noted that the mixtures with Retarder 2 were more sensitive to the change of curing temperature, and their set times decreased more rapidly than those of the mixtures with Retarder 1 as the curing temperature increased.

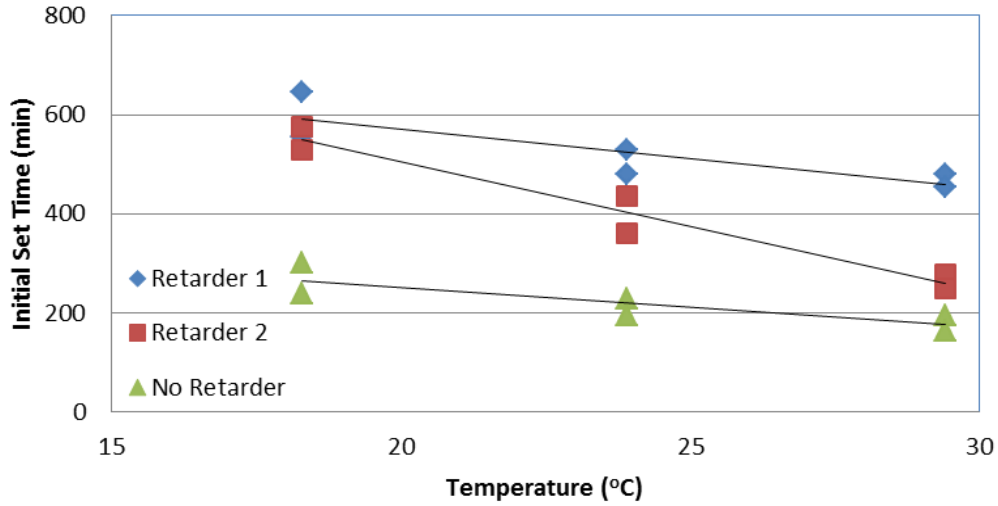

(a) Initial Set

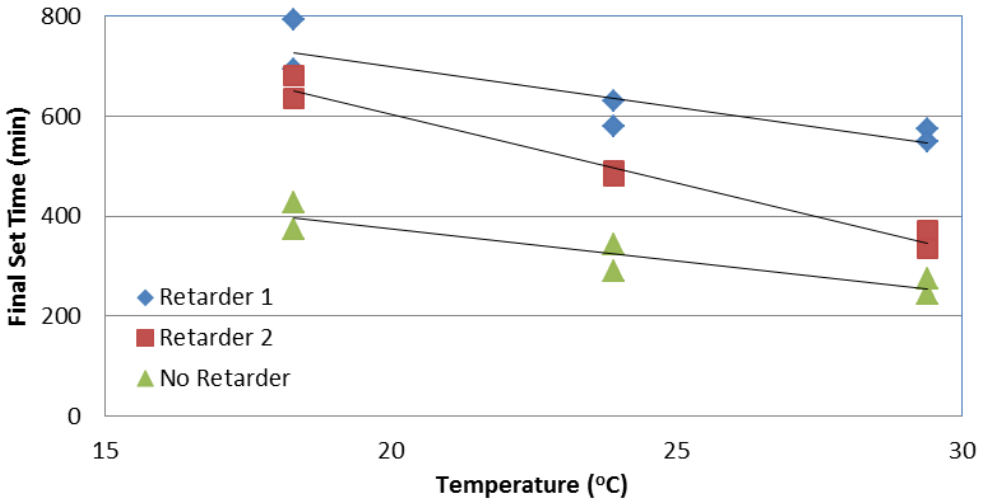

(b) Final Set

Figure 5. Effect of retarder type on concrete set time

Effect of Fly Ash Replacement

As expected, the 20% fly ash replacement for cement extended concrete initial/final set time due to its slow hydration process and water reducing effect. To

effectively evaluate the influence of the fly ash, the initial/final set times for concrete mixtures with fly ash replacement are normalized (or divided) by the set times of the corresponding concrete mixtures without fly ash replacement, and the results are listed in Table 6.

As seen in Table 6, the normalized initial set times for mixtures with different retarders under three different temperature conditions are very close, 1.15, while the normalized final set times for these mixtures are approximately equal to 1.10. Based on these results, when a new retarder is used in a concrete mixture, one can estimate the initial/final set times of the mixture with 20% fly ash replacement by testing initial/final set time for the mixture without fly ash replacement and multiplying the results with the factor of 1.15 or 1.10, respectively, thus, significantly reducing the number of set time tests required for construction operations.

Table 6. Normalized set times of concrete mixtures

	Temperature (^{o}C)	Normalized Set Time			
		Retarder 1	Retarder 2	No Retarder	Average
Initial	29.4	1.05	1.11	1.18	1.12
	23.9	1.10	1.21	1.18	1.16
	18.3	1.16	1.08	1.25	1.17
Final	29.4	1.05	1.10	1.12	1.09
	23.9	1.09	1.02	1.18	1.10
	18.3	1.14	1.07	1.14	1.12

Concrete Setting Behavior and Maturity

The maturity concept has been widely used to account for the effect of different curing temperatures on the strength development of concrete (4, 5). Since penetration

resistance is also related to concrete strength, a correlation between the penetration resistance and concrete maturity is expected.

According to ASTM C 1074, concrete maturity can be expressed as the time-temperature factor (TTF) based on the Nurse-Saul equation as shown below:

$$M \text{ or } TTF = \Sigma [(T_a - T_0)\, \Delta t] \qquad (3)$$

In this equation, M is the maturity; T_0, the datum temperature of concrete, below which the concrete has no strength gain; Δt, a time interval in terms of hours; and T_a, the average concrete temperature during Δt.

Table 7. Datum temperature used by State DOTs in United States

State DOTs	Specification	Datum Temp. (^oC)	State DOTs	Specification	Datum Temp. (^oC)
Alabama	ALDOT-425	0	Missouri	Section 507	-10
Indiana	ITM 402-04T	-10	Ohio	Supplement 1098	0
Iowa	IM 383	-10	Tennessee	Developing	-10
Kansas	KT-44	-10	Texas	Tex-426-A	-10
Kentucky	64-322-08	-10	Wisconsin	CMM 8.70	0

*Information updated in March 2012

The datum temperature (T_0) depends on the property of cement, fly ash and chemical admixture used, and it varies widely (6, 7). Table 7 presents the datum temperatures that are used by several state highway agencies, and it indicates that the

value of -10^{o}C is most commonly used (8). Iowa Department of Transportation currently uses -10^{o}C as the datum temperature for evaluating maturity of concrete pavement.

Using the temperature measurements shown in Figure 1 and the datum temperature of -10^{o}C, the TTF values of the concrete mixes studied were computed according to Equation (3). These values were then plotted against the penetration resistance of the corresponding concrete measured from the standard set time test (ASTM C 403). Figures 6 and 7 show the penetration resistance versus TTF curves for the concrete mixes with Retarder 1 and without retarder, respectively. Different from Figure 3 (penetration resistance vs. elapsed time), Figures 6 and 7 suggest that the penetration behavior of a concrete under different curing temperatures can be described by a single curve if the maturity concept was used. The significance of the maturity application here is to predict the penetration resistance for concrete cured under different temperatures.

When the above maturity method was also applied to the concrete mixtures containing Retarder 2, Figure 8 is obtained for the datum temperature of -10^{o}C. The three curves in Figure 8 suggest that the use of -10^{o}C datum temperature is not appropriate here. The datum temperature, related to cement hydration, is affected by the chemistry of cement system, and therefore, may change when different chemical admixtures are used. Figure 9 illustrates that a single penetration resistance-maturity relationship can be obtained when the datum temperature of 4^{o}C is used. This result indicates that a proper selection of the datum temperature is very important for the maturity application.

It shall be noted that although many state DOTs use the datum temperature of -10 ^{o}C, ASTM C 1074 (3) recommends a datum temperature of 0^{o}C for concrete used Type I cement and without chemical admixtures. Brooks (9) reported datum temperatures of -1.3 to 3.4^{o}C for concrete made with various SCMs. Johnson (10) suggested a datum temperature of 3.8 ^{o}C for Maryland DOT. Dong (11) recommended a datum temperature ranging from -2.0 ^{o}C to 4.5^{o}C for AKDOT. A datum temperature of 4^{o}C used in Figure 9 is within the range reported in literatures.

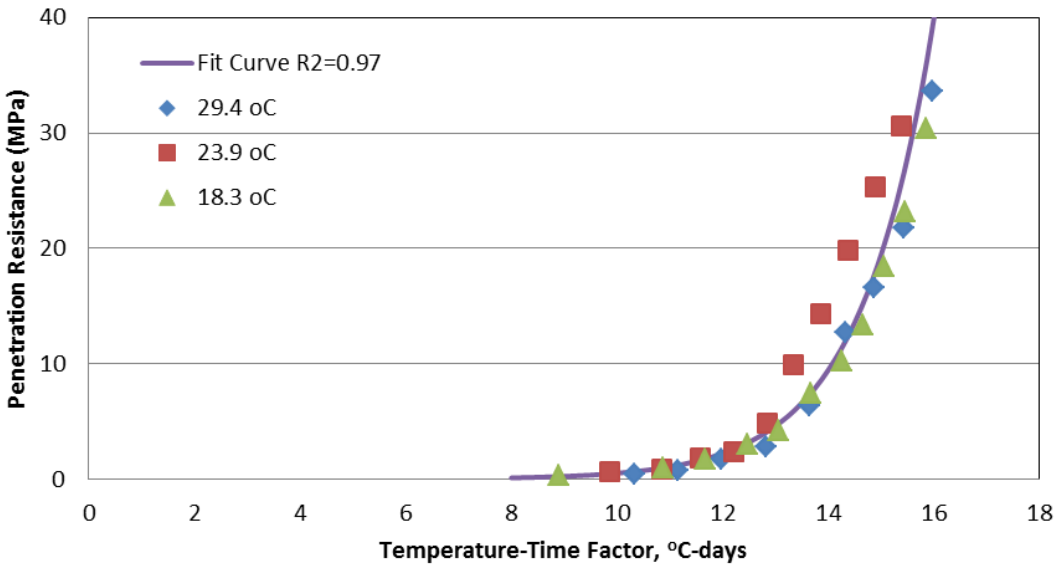

(a) With fly ash

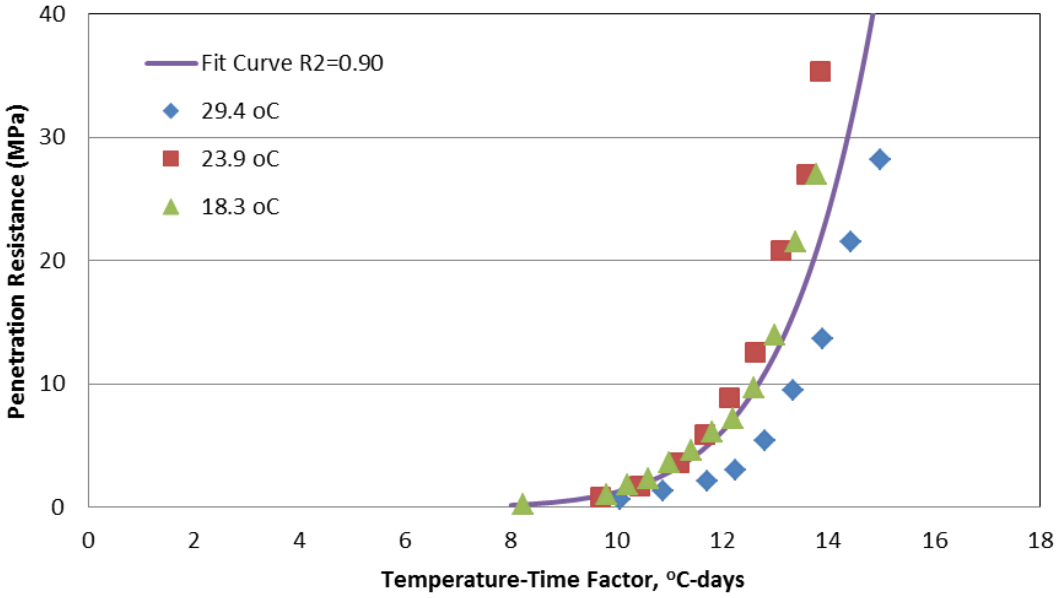

(b) Without fly ash

Figure 6. Penetration resistance-maturity relationship of mixtures with retarder 1 (T_0 = -10°C)

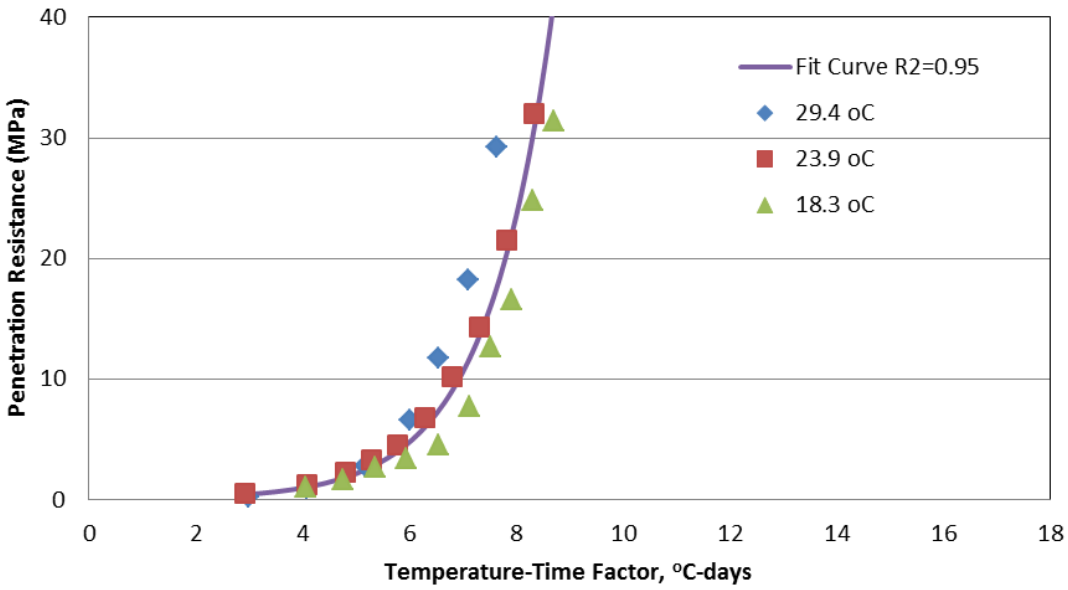

(a) With fly ash

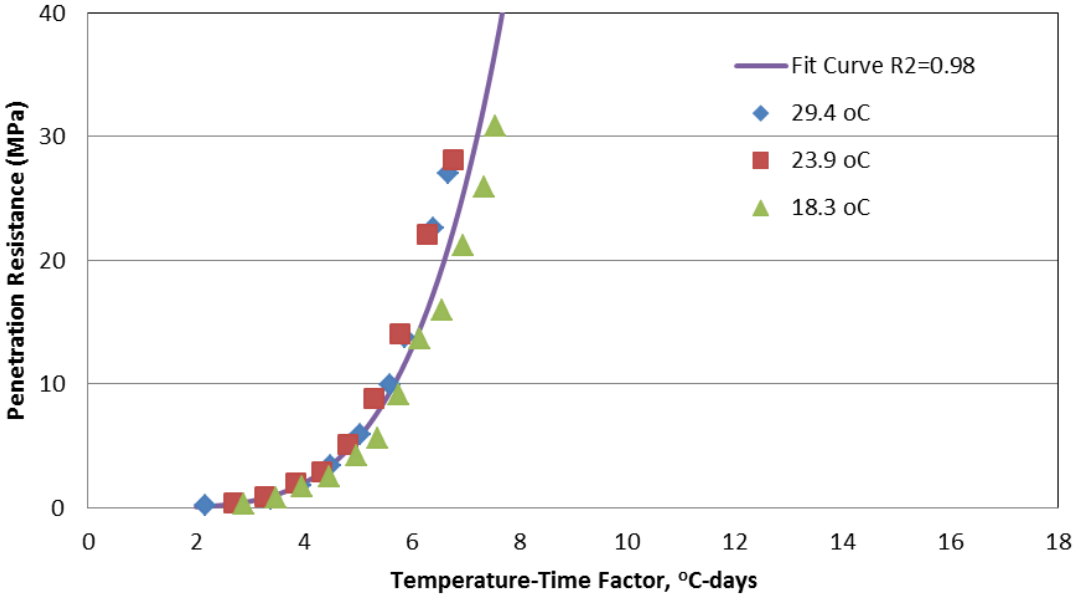

(b) Without fly ash

Figure 7. Penetration resistance-maturity relationship of mixtures without retarder (T_0 = -10°C)

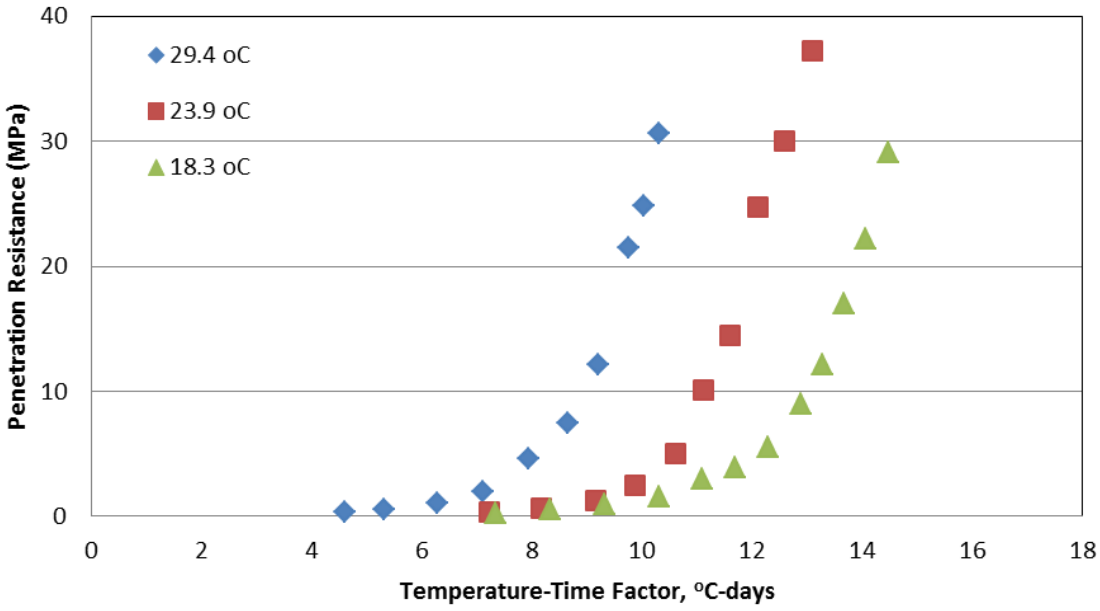

(a) With fly ash

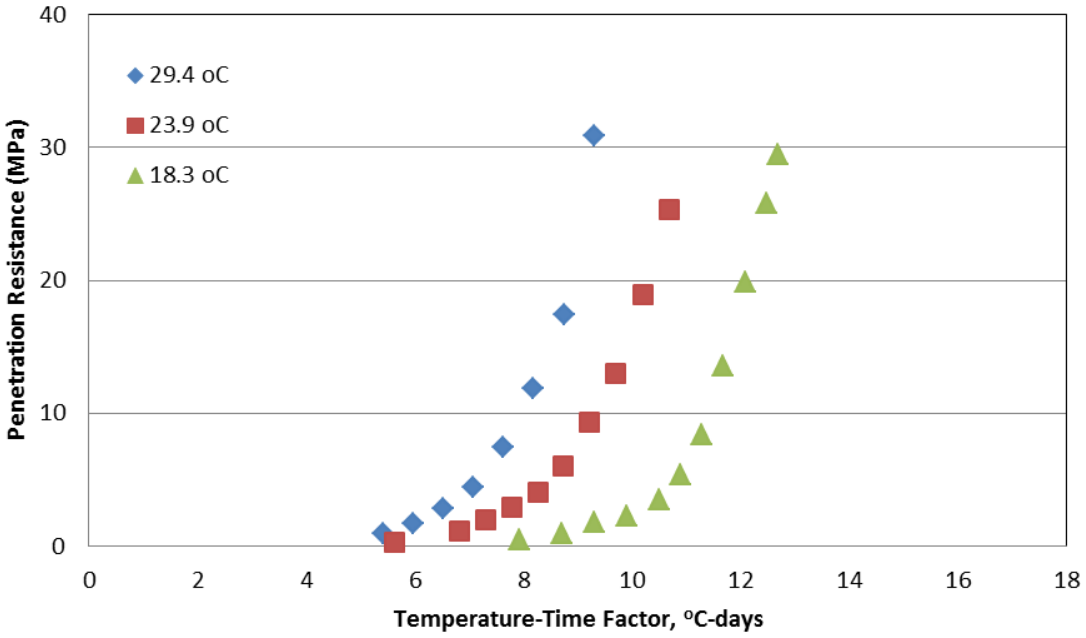

(b) Without fly ash

Figure 8. Penetration resistance-maturity relationship of mixtures with retarder 2 (T_0 = -10°C)

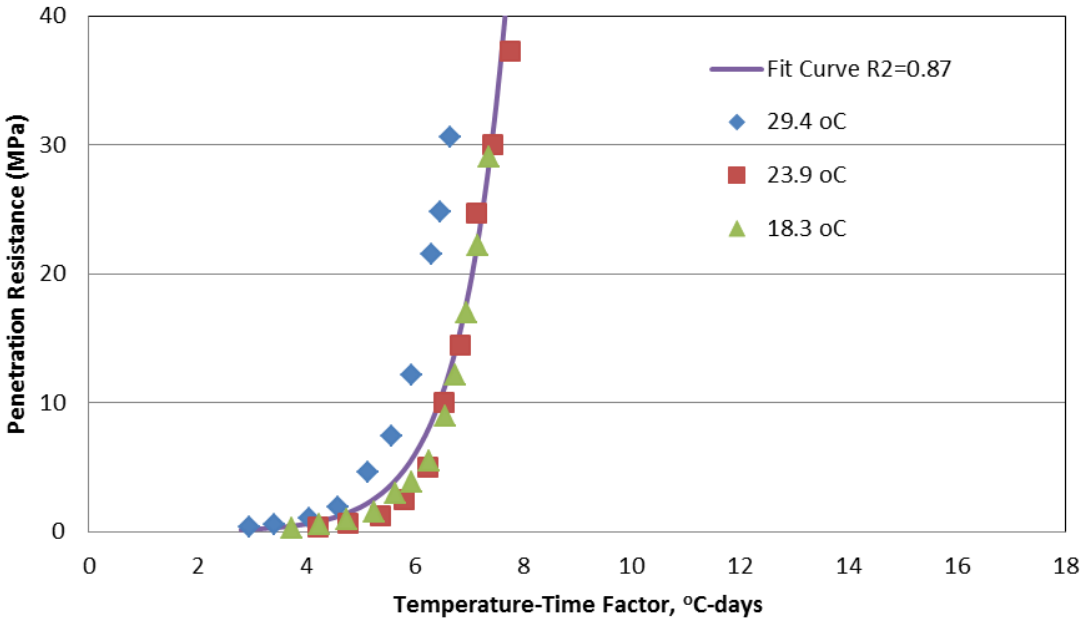

(a) With Fly Ash

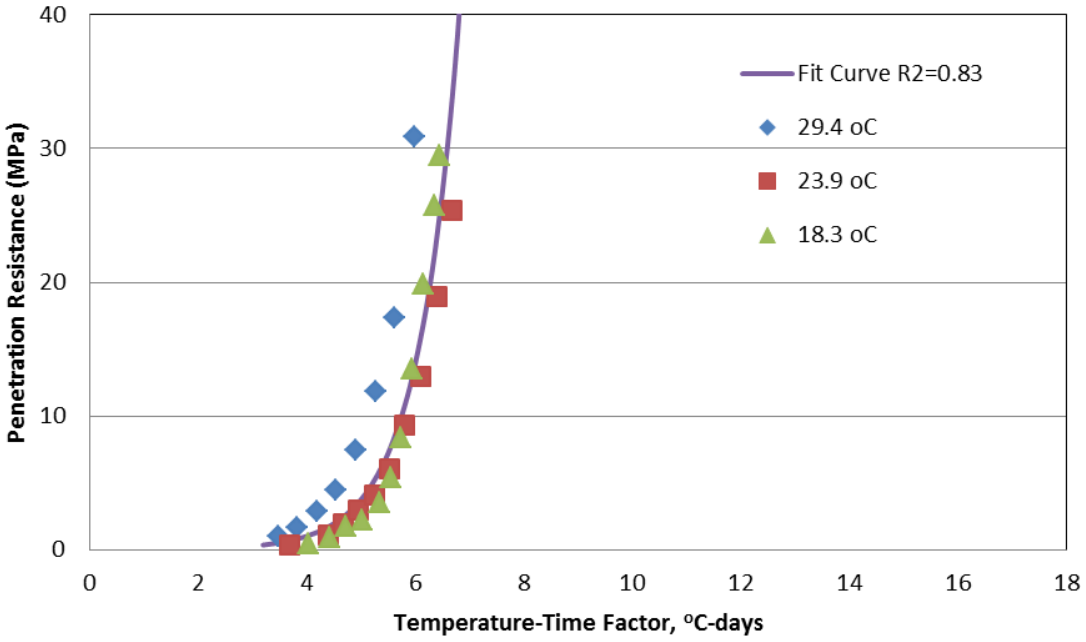

(b) without Fly Ash

Figure 9. Penetration resistance-maturity relationship of mixtures with retarder 2 ($T_0 = 4^oC$)

Conclusions

The maturity concept is used to describe the setting behavior or penetration resistance of concrete under different curing temperatures. It is found that concrete penetration resistance correlated well with its maturity, i. e. time-temperature factor (TTF), when the datum temperature of the concrete was properly selected. Once the relationship is established, one can predict the concrete penetration resistance by simply measuring the concrete maturity. Further study is needed to investigate the effect of chemical admixtures on datum temperature of concrete.

In addition, the study indicates that:

1. If curing temperature raises $1^{o}C$, the initial set time and final set time will drop about 15 min and 19 min, respectively.
2. Mixtures with Retarder 2 (sodium salt) are more sensitive with temperature changes.
3. The 20% fly ash replacement increases the concrete initial and final set times by a factor of approximate 1.15 and 1.10, respectively.

Acknowledgement

The supply of concrete materials and inputs on the test results from Iowa Department of Transportation are greatly acknowledged.

References

1. Jones, K. “Admixtures for Use as Retarders and Water Reducers in C-WR Mixes” MLR 8812, Materials Office, Iowa Department of Transportation, 1988.

2. ASTM C 403, “Standard Test Method for Time of Setting of Concrete Mixtures by Penetration Resistance”, the American Society of Testing and Materials, May 2008.

3. ASTM C 1074, “Standard Practice for Estimating Concrete Strength by the Maturity Method”, the American Society of Testing and Materials, May 2011.

4. Carino, N. J., “The Maturity Method, Theory and Application”, ASTM Journal of Cement, Concrete and Aggregates, Vol. 6, No. 2, Winter 1984, pp. 61-73.

5. Tank, R. C., and Carino, N. J., “Rate Constant Functions for Strength Development of Concrete,” ACI Materials Journal, Vol. 88, No. 1, January-February, 1991, pp. 74-83.

6. Carino, N. J. and Tank, R. C., “Maturity Functions for Concrete Made with Various Cements and Admixtures,” ACI Materials Journal, Vol. 89, No. 2, March-April, 1992, pp. 188-196.

7. Wang, K. and Ge, Z., “Evaluating Properties of Blended Cements for Concrete Pavements”, Ceneter for Portland Cement Concrete Pavement Technology, Iowa State University, Final Report, December 2003.

8. Mindess, S., Young, J. F., and Darwin, D., Concrete, 2nd Edition, Prentice Hall, Inc., NJ. 2003, 644 pp.

9. Brooks, G. A., Schindler, K. A., and Barnes, W. R., “Maturity Method Evaluated for Various Cementitious Materials”, Journal of Materials in Civil Engineering, December 2007

10. Johnson, R. and Hosten M. A., “Implementation of the Concrete Maturity Meter for Maryland”, Final Report, Morgan State University, November 2011

11. Dong, Y., Song, R. and Dhungana, J., “Study of Concrete Maturity in Very Cold Weather”, Final Report, Institute of Northern Engineering, University of Alaska, Fairbanks, December 2009

CHAPTER 3. A SIMPLE STATISTICAL MODEL FOR PREDICTION OF SHRINKAGE BEHAVIOR OF HIGH PERFORMANCE CONCRETE CONTAINING SUPPLEMENTARY CEMENTITIOUS MATERIALS

A paper to be submitted to Journal of Construction and Building Materials

Qizhe Hou, Kejin Wang and Yu Chen

Abstract

In this paper, autogenous shrinkage and free drying shrinkage of nine different high performance concrete mixes, commonly used for bridge decks and bridge overlays constructions, were measured. The mixtures were systemically designed for evaluating effects of class C fly ash and ground granulated blast-furance slag replacement. An exponential model was introduced for describing and predicting shrinkage in high-performance concrete when different types and amounts of supplementary cementitious materials were used. This model fits for both autogenous and free drying shrinkage and is validated and proved by comparing measured value with predicted shrinkage value of an independent group of mixtures. The effects of supplementary cementitious materials on concrete shrinkage behavior were also evaluated.

1. Introduction

High-performance concrete (HPC) is widely used for the construction of bridge decks and overlays due to its attractive material properties, including high strength, fast strength development, low permeability, and excellent durability. However, due to its

high paste content, low water-to-binder ratio (w/b), and chemical admixtures, HPC generally has considerably higher autogenous shrinkage than normal strength concrete (NSC), which may have significant contribution to the total shrinkage of the concrete. .

For normal concrete, autogenous shrinkage is generally low, and therefore it doesn't significantly contribute to the total shrinkage of the concrete. For high-performance concrete, with a water-to-cement ratio less than 0.4 or compressive strength larger than 8700 psi, the autogenous shrinkage is relatively high and shall be considered as a part of total shrinkage. (1)

Some supplementary cementitious materials (SCMs), such as slag, have mixed effects on autogenous shrinkage and free drying shrinkage. Thus, the present study focuses on investigating the total shrinkage (define as autogenous shrinkage plus free drying shrinkage) of high performance concrete, when different type and amount of (SCMs) are used. Therefore, total shrinkage has been used to indicate the shrinkage properties of high performance concrete in this study.

A sufficient model for predicting total shrinkage in high-performance concrete is essential for cracking control. The existing models for prediction of concrete shrinkage by using factors such as specimen volume-to-surface ratio, relative humidity, cementitious material type and content, water-to-cement ratio, aggregate content, and admixtures, therefore, are always complicated. The latest and most commonly used models provided by American Concrete Institute, such as ACI 209R-92, B3, CEB MC90, CEB MC90-99, and GL2000, are based on experimental data.(1) Since those empirical models focus on predicting shrinkage that fits the most mix compositions and

environmental conditions, for a particular mix composition there is always a lack of accuracy. (2) Additionally, those models always focus on concrete mixtures with little or no replacement by (SCMs), and there are limitations for concrete admixtures with high percentage of SCMs such as silica fumes, slag, and fly ash. (1) Based on those observations, a simplified model is needed to predict the shrinkage of concrete with high percentage of SCMs such as fly ash and slag.

In the present study, the exponential model demonstrates a different approach to predict autogenous and free drying shrinkage of high-performance concrete by using only one general equation. Model coefficients indicate the physical meaning such as ultimate shrinkage (shrinkage at 56 days), rate of shrinkage at different age period. After the model simplification and calibration, an exponential model for both autogenous and free drying shrinkage can be achieved with only two model coefficients.

2. Materials

The experiments were designed to characterize the properties of free drying shrinkage and autogenous shrinkage of seven high-performance concrete mixtures. Two types of SCMs (class C fly ash and ground granulated blast furnace slag) were used to systemically study of the effects of different types and amounts of SCMs on the autogenous and free drying shrinkage of mortar. The experiments were conducted at the standard conditions according to ASTM C596 and ACI 209.2R-08 to minimize model parameters. To simulate concrete, the mix proportions of mortar were basically the same as those of high-performance concrete, except that no coarse aggregate was added.

Table 1 presents the nine high-performance concrete mix proportions that were recommended by the Iowa Department of Transportation (Iowa DOT). Mixture ID PC' and 20F' are independent samples designed for model validation purpose; therefore, the mix proportions such as cement and sand content, type and dosage of chemical admixtures are different from others. For the first seven mixtures, an air entraining agent, a mid-range water reducer, and a retarder were used as chemical admixtures for this study. 0.4 water-to-binder ratio and 1.98 sand-to-binder ratio are applied for those seven mixtures as well.

Table 1. Mix Proportions of Mortar (per cubic yard)

ID	Cement type I/II	Fly Ash (slag)	Sand	s/b	Water	w/b	AEA	MRWR (NRWR)	Retarder
	lbs	lbs	lbs		lbs		ml	ml	ml
PC	709	-	1404	1.98	284	0.4	378	1259	419
25S	532	(177)	1404	1.98	284	0.4	378	1259	419
35S	461	(248)	1404	1.98	284	0.4	378	1259	419
45S	390	(319)	1404	1.98	284	0.4	378	1259	419
10F	638	71	1404	1.98	284	0.4	378	1259	419
20F	567	142	1404	1.98	284	0.4	378	1259	419
30F	496	213	1404	1.98	284	0.4	378	1259	419
PC'*	666	-	1406	2.11	267	0.4	354	(708)	394
20F'*	459	115	1486	2.59	241	0.42	378	(610)	348

* Type IP cement, normal-range water reducer (NRWR)

3. Test Methods

3.1. Test Method for Autogenous Shrinkage

Autogenous shrinkage test of mortar is performed according to ASTM C 1698 and each mixture three samples (Ø 30×L300 mm corrugated polyethylene mold) are prepared. Fill the corrugated mold with mortar and seal each ends properly. After the specimens were made, place them horizontally on a smooth surface to avoid any unexpected length change due to its gravity. Place the specimens into the environmental chamber and keep the ambient temperature at 73±4 ^{o}F. The final setting time should be determined in advance according to ASTM C403/C403M, since it is the exact moment for the first measurement. The specimen preparation process is shown as figure 1.

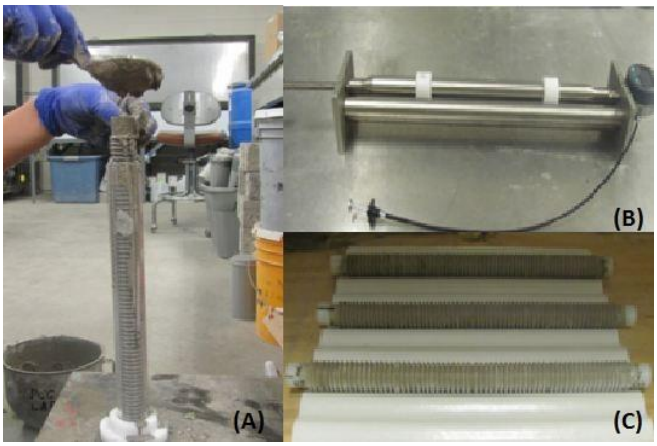

(a) specimen preparation (b) testing device (c) specimens storage

Figure 1. Specimen preparations for autogenous shrinkage of mortar

3.2. Test Method for Free Drying Shrinkage

Free drying shrinkage test of mortar is performed according to ASTM C 596 and three specimens (25×25 ×285mm) are made for each mixture. Moist cure the specimens

with 100% relative humidity for 1 day and then place them into lime-saturated water storage for 2 days. At the age of 72±0.5h, remove the specimens from water and then placed in the environment room with 73±4 ^{o}F and 40% relative humidity for drying storage. The initial length measurements are immediately taken after the specimens are removed from water. The test device and specimens of free drying shrinkage of mortar is shown in figure 2.

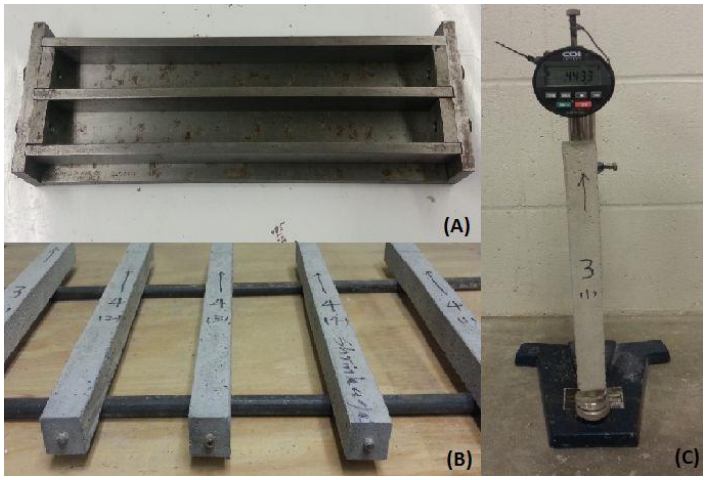

(a) shrinkage mold (b) specimens storage (c) testing device

Figure 2. Test device and specimens of free drying shrinkage of mortar

4. Test Results and Analysis

4.1. Typical Measurement

Figure 3(a) and 3(b) illursate typical measurements of autogenous shrinkage and free drying shrinkage of a set of three specimens. As shown in the figures, the variations in the measurements of the three samples are very small. Thus, the average of the three samples can be used to represent consistent and reliable results.

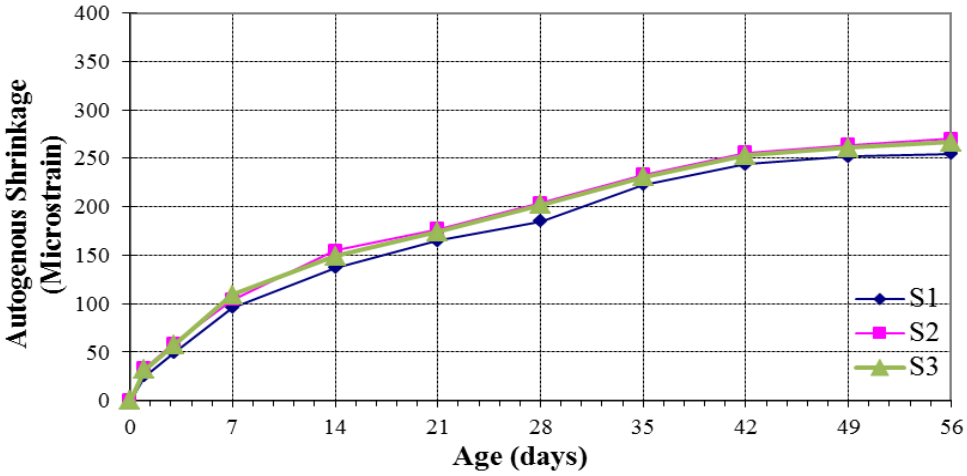

Figure 3(a). Typical autogenous shrinkage measurements of 25% Slag

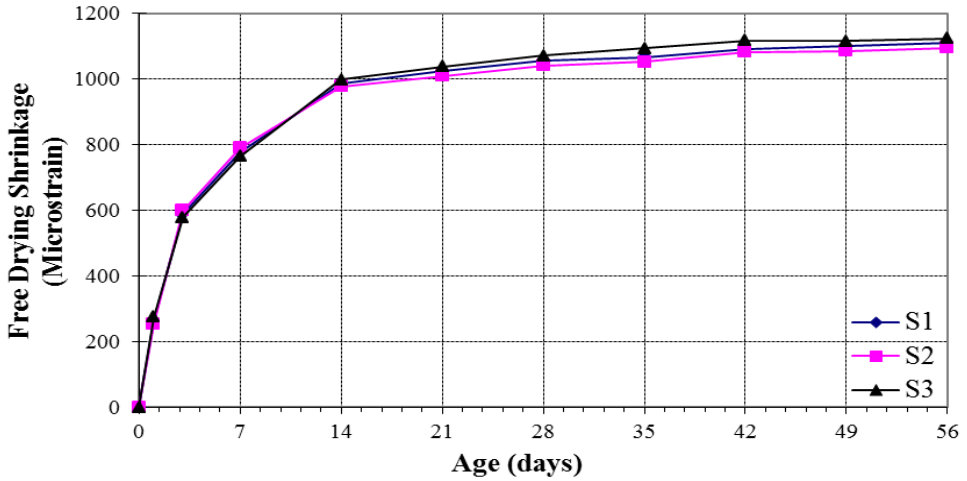

Figure 3(b). Typical free drying shrinkage measurements of 25% Slag

4.2. Autogenous Shrinkage of Mortar

The effects of SCMs on autogenous shrinkage vary depending on the type and amount of the replacement added to the mixture, calculated as a percentage of the whole. The addition of ground granulated blast furnace GGBF slag was found to increase the autogenous shrinkage, as shown in Figure 3. Referring to the figure, the results of a

series of tests using different replacement percentages show that greater GGBF slag content led to an increase in autogenous shrinkage. Compared to the control mixture, the GGBF slag mixtures had higher paste content due to the low specific gravity of GGBF slag; therefore, they contributed more autogenous shrinkage. (6)

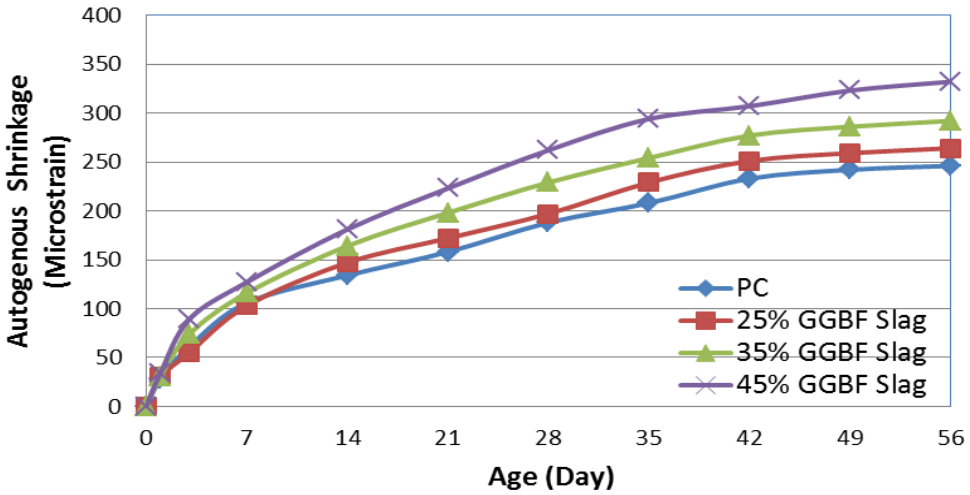

Figure 4(a). Effect of GGBFS on autogenous shrinkage of mortar

However, on the contrary, the addition of fly ash (FA) caused a reduction of the autogenous shrinkage. Figure 4 presents the effect of FA on the autogenous shrinkage of mortar. As the FA content increased up to 30%, the ultimate autogenous shrinkage was reduced as much as 22%. This was due to the chemical expansion of the cement paste. (7)

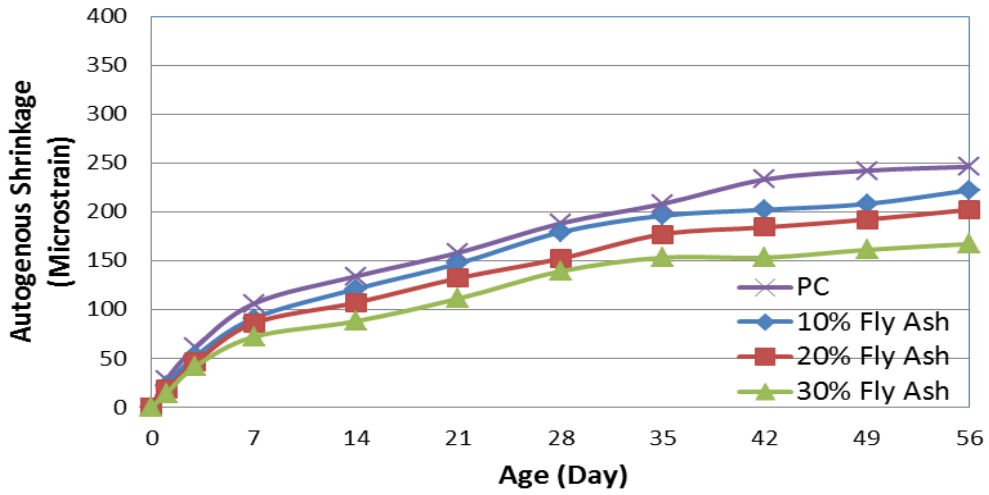

Figure 4(b). Effect of fly ash on autogenous shrinkage of mortar

4.3. Free Drying Shrinkage of Mortar

The addition of GGBF slag increased free drying shrinkage after seven days of drying, but it lowered the shrinkage as the material aged. Figure 5 illustrates the highest GGBFS replacement mixture leading a highest shrinkage value at early age and the lowest shrinkage value after 56 days of drying. As mentioned previously, GGBF slag mixtures have higher paste content; therefore, they contribute more shrinkage at the early age. After several days of drying, the pozzolanic reaction of GGBF slag enhanced the strength of the concrete pore structure and improved the deformation resistance. (8)

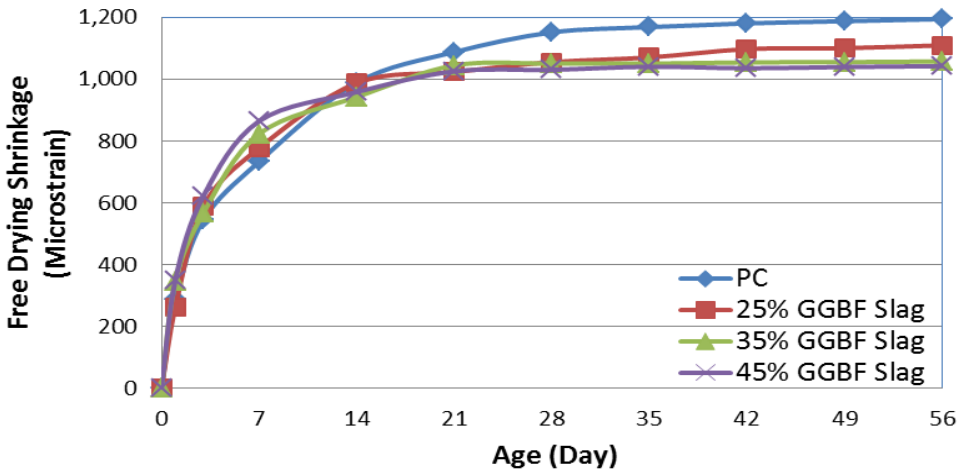

Figure 5(a). Effect of GGBFS on free drying shrinkage of mortar

Figure 6 shows a clear relationship between the percentage of fly ash replacement and reduction of free drying shrinkage. Similar to autogenous shrinkage, as the fly ash content increased up to 30%, the ultimate free drying shrinkage was reduced as much as 21%. For the application purpose, the addition of fly ash replacement can lower the water requirement, and therefore reduce the free drying shrinkage. (7) Thus, fly ash was evaluated as a good SCM to reduce both types of shrinkage.

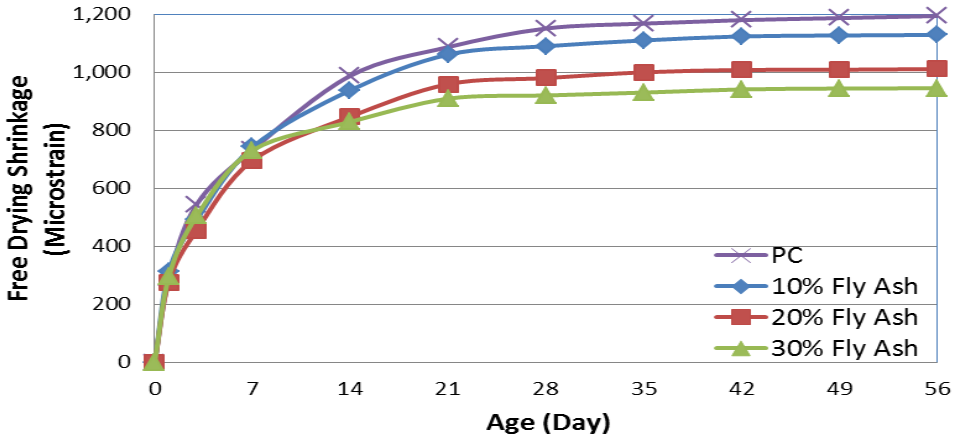

Figure 5(b). Effect of fly ash on free drying shrinkage of mortar

4.4. Total Shrinkage of Mortar

The total shrinkage of mortar, defined as the autogenous shrinkage plus free drying shrinkage, is shown in figure 6. As shown in figure 6(a), the curves with slag replacements were overlapped during the 56 day of measurement, which indicates the GGBF Slag has no significant effect on total shrinkage. Figure 6(b) presents the effect of fly ash on total shrinkage. The curves were overlapped at the beginning; however, after 7 days, with the increase of fly ash replacement rate, the total shrinkage was reduced.

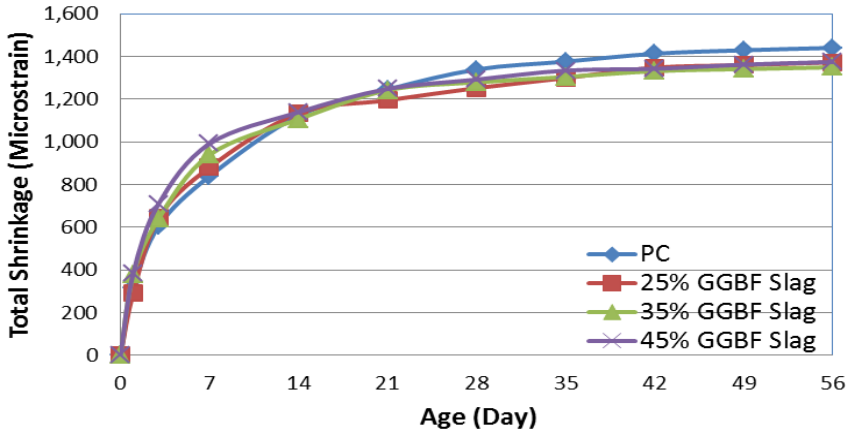

Figure 6(a). Effect of GGBFS on total shrinkage of mortar

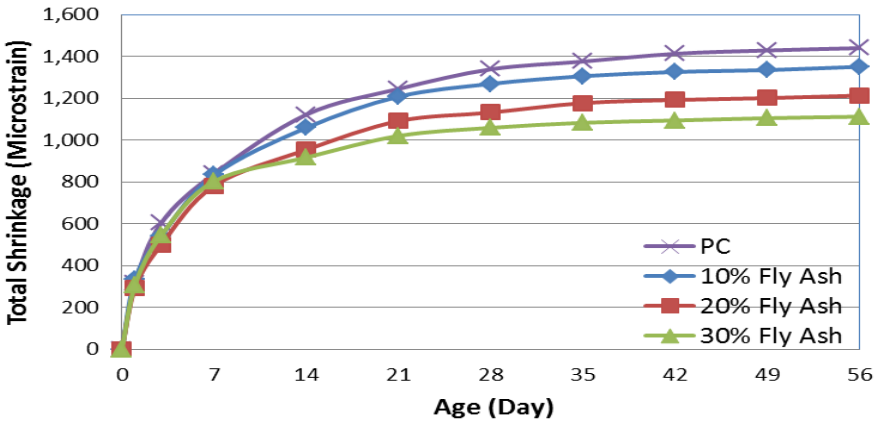

Figure 6(b). Effect of fly ash on total shrinkage of mortar

4.5. Relationship between Free Drying Shrinkage and Autogenous Shrinkage

Figure 7 below illustrates free drying shrinkage versus autogenous shrinkage for all seven mixtures. The mixture with 30% FA replacement had the lowest autogenous shrinkage and free drying shrinkage. The mixture with 45% GGBF slag had the highest autogenous shrinkage, and the control mixture had the highest free drying shrinkage. As the FA content decreased, both autogenous and free drying shrinkage increased. However, as the GGBF slag content decreased, only the autogenous shrinkage was decreased.

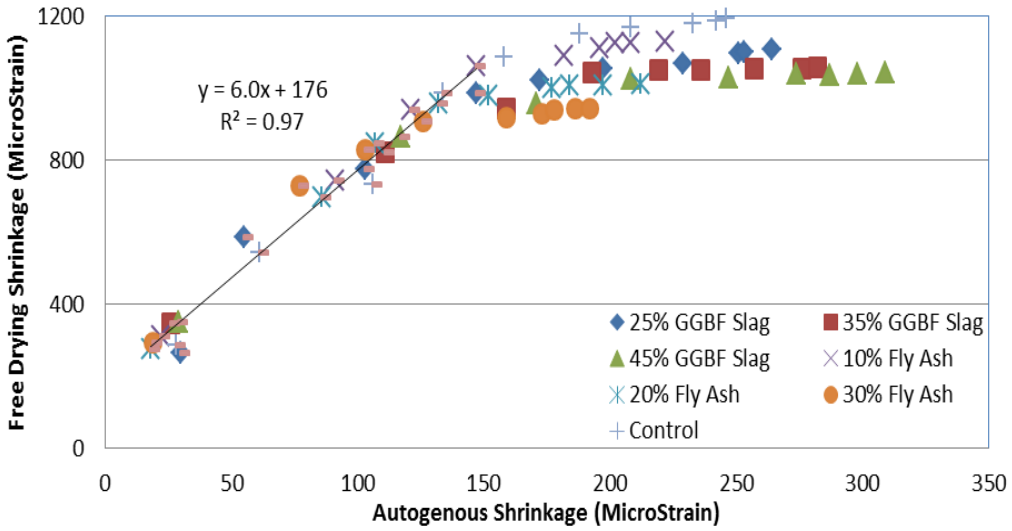

Figure 7. Free drying shrinkage vs. autogenous shrinkage

A linear relationship between autogenous shrinkage and free drying shrinkage was observed at 14 days of drying, with autogenous shrinkage of 150 microstrain and free drying shrinkage of 1000 microstrain. As Figure 7 shows above, the linear regression equation was found to have an R square of 0.97. This relationship can be used to estimate shrinkage at early ages without considering the type and amount of SCMs

added to the mixture when one of the shrinkage types is known. However, after 14 days the overall linear relationship has disappeared and each mixture behaves differently. It indicates that SCMs affect the shrinkage properties mostly after the age of 14 days.

5. A Statistical Model for Shrinkage Prediction

5.1. Model Development

Shrinkage models CEB MC90-99 and JSCE Specification 2002 subdivide the total shrinkage into autogenous shrinkage and free drying shrinkage for high-performance concrete. (5, 9) The total shrinkage can be calculated from Equation 1 below:

$$\varepsilon_{total}(t) = \varepsilon_{auto}(t) + \varepsilon_{drying}(t) \qquad \text{(Eq 1)}$$

Where t is the age of mortar (days), $\varepsilon_{total}(t)$ is the total shrinkage ($x10^{-6}$ m/m or microstrain) at the age of t (days), $\varepsilon_{auto}(t)$ and $\varepsilon_{drying}(t)$ are the autogenous shrinkage (microstrain) and free drying shrinkage (microstrain) respectively at the age of t (days). An exponential 3P model for predicting autogenous shrinkage and free drying shrinkage was developed based on the experimental data. Figure 8 below shows a typical nonlinear exponential 3P fitting model for the autogenous shrinkage of mixture with 10% FA analyzed by statistic software package. This exponential model can be applied to the free drying shrinkage as well.

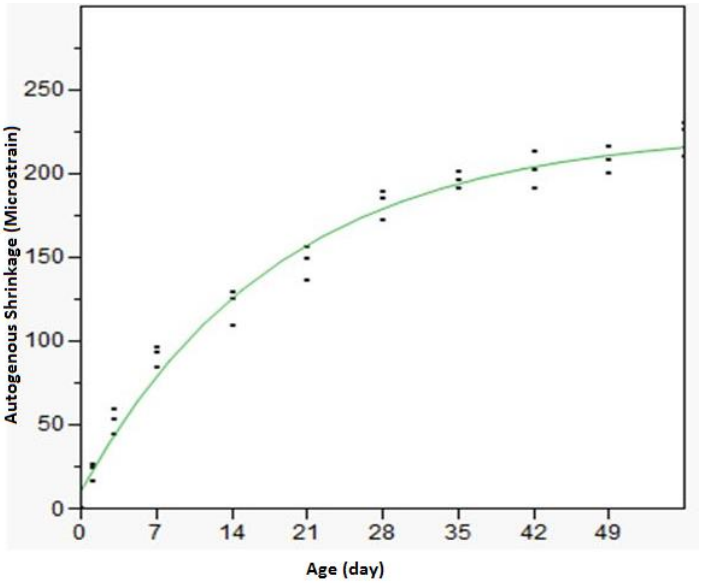

Figure 8. Typical curve fitting for autogenous shrinkage of mixture with 10% fly ash replacement

Equation 2 below presents the general form of the autogenous and free drying shrinkage model:

$$\varepsilon_{auto/drying}(t)=a+b*e^{(c*t)} \qquad \text{(Eq 2)}$$

where a (Asymptote), b (Scale) & c (Growth Rate) are model coefficients, t presents the mortar age within 56 days, $\varepsilon_{auto/drying}$ presents shrinkage (microstrain) at the corresponding age of t.

The physical meaning of a (Asymptote), b (Scale) and c (Growth Rate) are ultimate shrinkage (shrinkage at 56 days), rate of shrinkage between 0 and 7 days and rate of shrinkage between 7 and 21 days respectively. Refer to the equation 2, if age (t) approaches 56 days, $b*e^{(c*t)}$ gets close to 0, and therefore the asymptote (a) is more likely equal to ultimate shrinkage. If scale (b) increased, the rate of shrinkage at early

age increased as well. If the growth rate (c) increase, the rate of shrinkage at middle age decreases.

Table 2 below presents the model coefficients for different types and amounts of replacement SCMs.

Table 2. Regression coefficients for modeling shrinkage of mortar

Shrinkage Type	Model Parameter	PC (Control)	10% FA	20% FA	30% FA	25% Slag	35% Slag	45% Slag
Drying	Asymptote (a)	1171	1113	996	924	1072	1042	1024
	Scale (b)	-1090	-1037	-935	-876	-1031	-984	-986
	Growth Rate (c)	-0.14	-0.15	-0.17	-0.23	-0.21	-0.24	-0.3
Auto	Asymptote (a)	262	226	222	202	280	290	322
	Scale (b)	-245	-215	-209	-192	-266	-275	-305
	Growth Rate (c)	-0.05	-0.05	-0.04	-0.05	-0.05	-0.05	-0.05

The parameters a (asymptote), b (scale), and c (growth rate) varied depending on the type and amount of SCMs. As figure 9 shows below, linear relationships between the model coefficient and percentage of SCM replacement were observed for all the parameters with both types of shrinkage, except the growth rate for autogenous shrinkage (use -0.05). It is certain that a greater asymptote value directly causes the higher ultimate shrinkage. Additionally, a combination of increased scale and decreased growth rate caused the slope to rise.

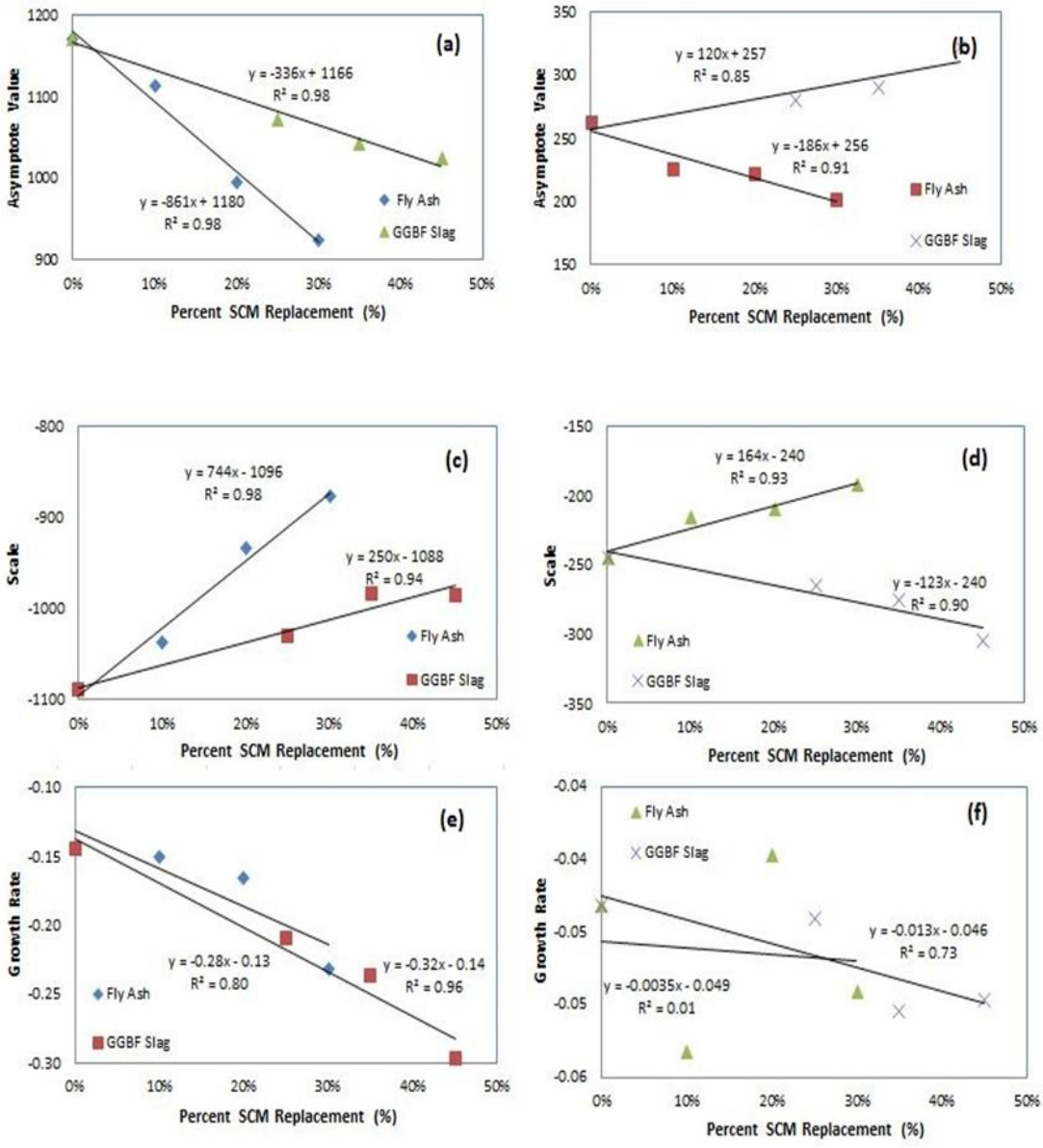

(Free Drying Shrinkage) **(Autogenous Shrinkage)**

Figure 9a to 9f: Relationship between model coefficients and SCM replacement

5.2. Model Simplification and Calibration

A linear relationship was found between the model coefficients asymptote (a) and scale (b) as seen in the figure 10 below:

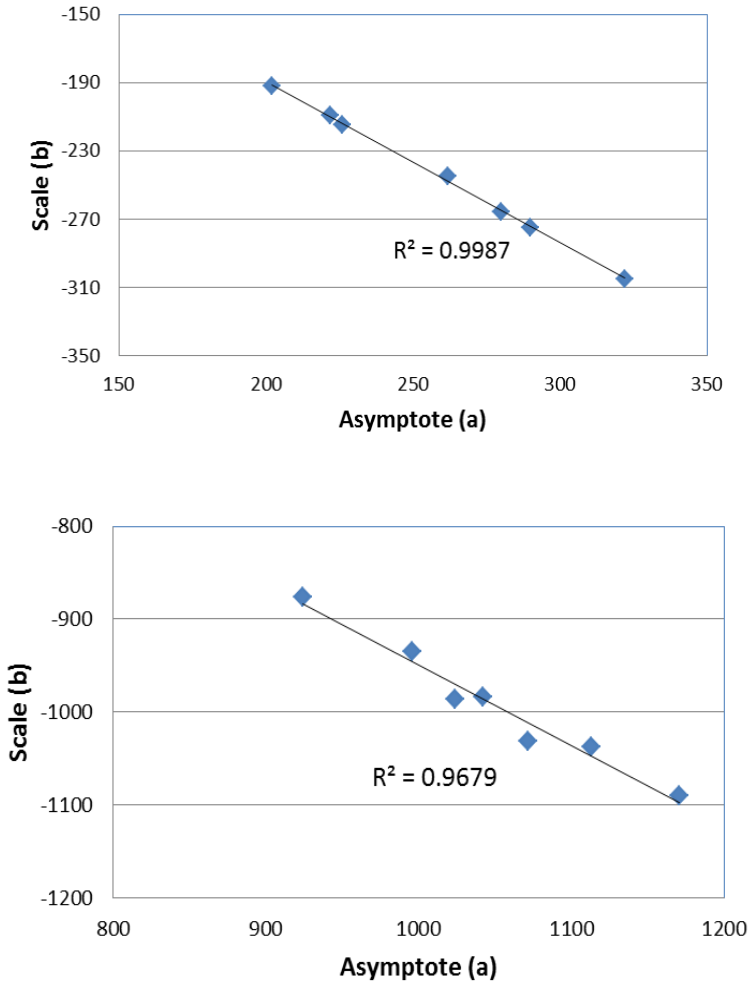

Figure 10. Scale vs. Asymptote for autogenous and free drying shrinkage

Thus, the correlation between asymptote and scale can be presented as in equation 3 below:

$$b = -0.95 * a \qquad \text{(Eq 3)}$$

Table 3 below presents the asymptote, measured ultimate shrinkage and predicted ultimate shrinkage by using equation 2 with corresponding model coefficients in table 2. It is certain that the model always predicted a lower ultimate shrinkage than measured.

Table 3 Ultimate shrinkage prediction

Type	Ultimate ε (microstrain)	PC (Control)	10% FA	20% FA	30% FA	25% Slag	35% Slag	45% Slag
Drying	Asymptote	1171	1113	996	924	1072	1042	1024
	Measured ε_{uult}	1194	1129	1011	945	1109	1057	1042
	Predicted ε_{ult}	1170.6	1112.8	995.9	924	1072	1042	1024
Auto	Asymptote	262	226	222	202	280	290	322
	Measured ε_{ult}	246	222	212	192	264	282	309
	Predicted ε_{ult}	247.1	212.9	199.8	190.3	263.8	273.3	303.5

The asymptote was calibrated and defined as follows:

$$a_{auto} = \varepsilon_{auto,ult} \qquad \text{(Eq 4)}$$

$$a_{drying} = \varepsilon_{drying,ult} \qquad \text{(Eq 5)}$$

Relative shrinkage (RS) was defined as the ultimate autogenous/free drying shrinkage ratio of a mixture with SCM replacement to the same mixture without SCM, as Equation 6 shows:

$$RS = \frac{\varepsilon_{ult,scm}}{\varepsilon_{ult,control}} \qquad \text{(Eq 6)}$$

The value of relative shrinkage and the percent SCM replacement were highly correlated, by plotting RS vs. percentage SCMs replacement according to the figure 11 shown.

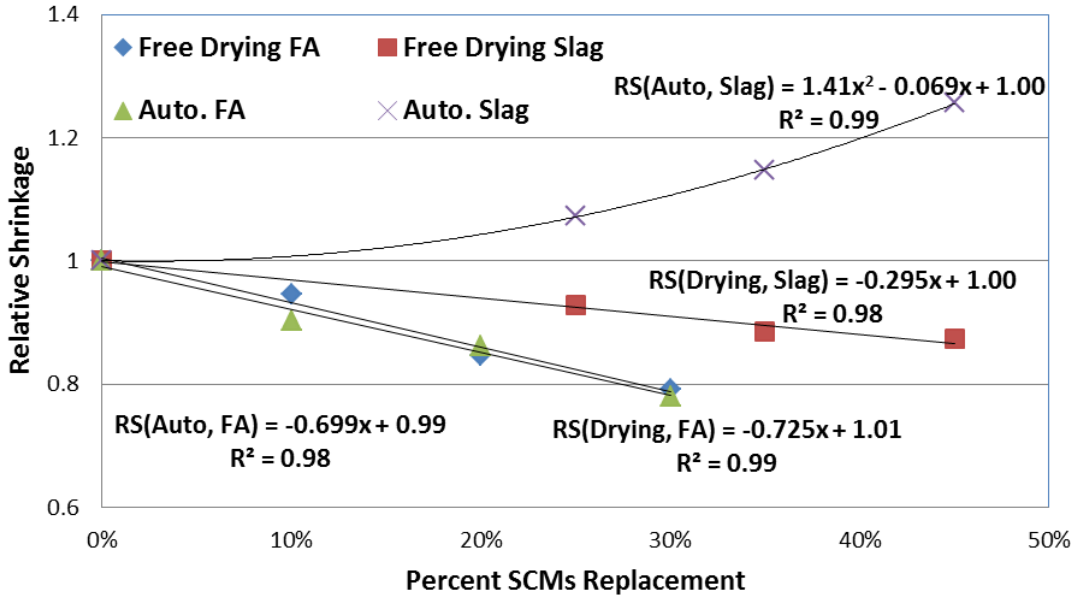

Figure 11. Relative shrinkage vs. percent SCMs replacement

Based on the above equations, the shrinkage prediction equations were rewritten as follows:

$$\varepsilon_{auto}(t) = RS^* \varepsilon_{auto,ult,control}^*[1-0.95*e^{(c*t)}] \quad \text{(Eq 7)}$$

$$\varepsilon_{drying}(t) = RS^* \varepsilon_{drying,ult,control}^*[1-0.95*e^{(c*t)}] \quad \text{(Eq 8)}$$

where $\varepsilon_{auto,ult,control}$ and $\varepsilon_{drying,ult,control}$ are shrinkages (microstrain) for mixtures without SCM at the age of 56 days. For a specific mix composition, the relative shrinkage (RS) and growth rate (c) are recommended and shown in figure 11 and figure 12 below:

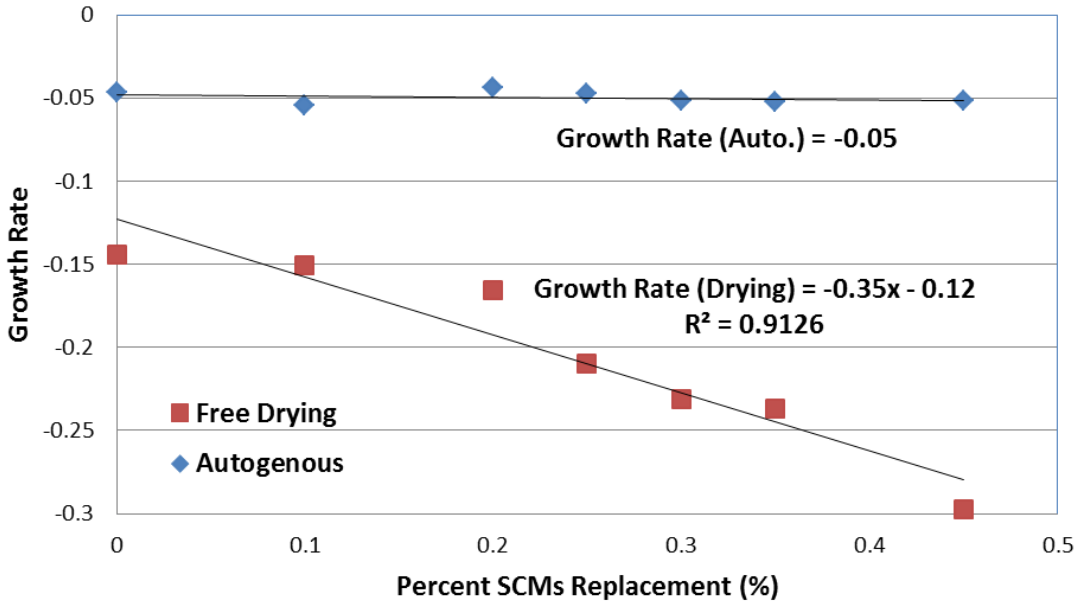

Figure 12. growth rate vs. percent SCMs replacement (%)

5.3. Model Testing

A total shrinkage for a specific mix composition with a certain amount of FA and GGBF slag replacement at any age within 56 days can be predicted if the ultimate shrinkage of both autogenous and free drying shrinkage for that mixture without SCM is known. To validate this model, shrinkage strains of an independent group of high-performance concrete were measured. The equation 7 and 8 were used to predict the both type of shrinkage within 56 days, and model coefficients were selected based on table 4. Figure show relationship between measured and predicted shrinkage.

As seen from the figures below, the shrinkage data points close to the line y=x, especially at the ultimate age. Therefore, the model is sufficient.

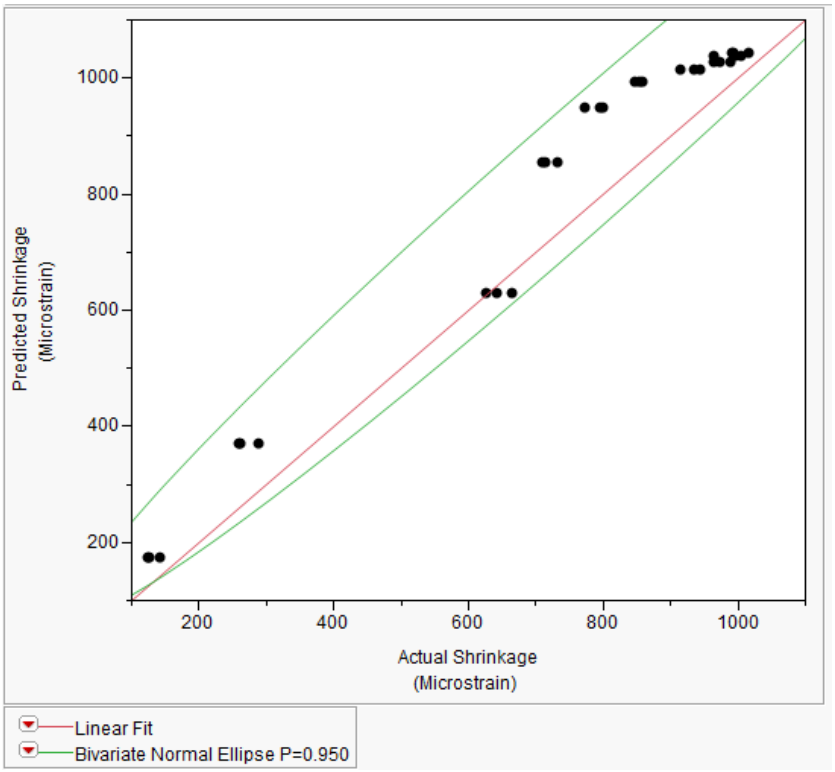

Figure 11. Predicted vs. actual shrinkage of total shrinkage

6. Conclusions

This paper presented experimental investigations of autogenous shrinkage and free drying shrinkage under the effects of SCMs such as GGBF slag and class C fly ash. Total shrinkage, defined as autogenous shrinkage plus free drying shrinkage, was used to represent the overall shrinkage properties of high performance concrete. A statistic model was developed and tested based on the experimental data, and was used to describe and predict both autogenous and free drying shrinkage. From the obtained results, the following conclusions can be made:

1. FA replacement can reduce both autogenous shrinkage and free drying shrinkage; therefore, reduce the total shrinkage of high-performance concrete.
2. Addition of GGBF slag increases the autogenous shrinkage, but reduces the free drying shrinkage. Thus, has no significant effect on total shrinkage.
3. A clear linear relationship between autogenous shrinkage and free drying shrinkage (Free drying shrinkage=6*autogenous shrinkage+176) is observed at the age between 0 and 14 days.
4. The exponential model, $\varepsilon_{auto/drying}(t)=a+b*e^{(c*t)}$, well describes both autogenous and free drying shrinkage (at any age of t) of the high-performance concrete studied.

References

1. ACI Committee 209, Guide for Modeling and Calculating Shrinkage and Creep in Hardened Concrete, American Concrete Institute, ACI 209.2R-08, 2008.
2. Will Hansen, Constitutive Model for Predicting Ultimate Drying Shrinkage of Concrete, J. Am. Ceram. Soc., 70[5] 329-32 (1987)
3. Shiho Kawashima and Surendra P. Shah (2010), "Early-age autogenous and drying shrinkage behavior of cellulose fiber-reinforced cementitious materials," Cement and Concrete Composites 33 (2011) 201-208
4. Rougelot, T., Skoczylas, F., and Burlion, N. (2009), "Water desorption and shrinkage in mortars and cement pastes: experimental study and poromechanical model," Cement and Concrete Research, vol. 39: 36-44.

5. Sakata K., and Shimomura T., Resent Progress on and code Evaluation of Concrete Creep and Shrinkage in Japan, Journal of Advanced Concrete Technology, 2(2), 113-140, 2004.

6. ACI Committee 226, “Ground Granulated Blast-Furnace Slag as a Cementitious Constituent in Concrete,” American Concrete Institute, ACI 226.1R-87, ACI Materials Journal, Vol. 84, No. 4, 1987, pp.327-342

7. Tangtermsirikul, S., “Class C Fly Ash as a Shrinkage Reducer for Cement Paste,” ASTM Special Publication, American Society for Testing and Materials, Volume 153, 1995.

8. Li J., and Yao Y., “A study on creep and drying shrinkage of high performance concrete,” Cement and Concrete Research, 31(8), 1203-1206, 2001

9. CEB, 1999, “Structural concrete-Textbook on Behavior, Design and Performance. Updated Knowledge of the CEB/FIP Model Code 1990, ” fib Bulletin 2, V. 2, Federation International, Lausanne, Switzerland, pp. 37-52.

10. E. Tazawa and S. Miyazawa (1995), “Influence of cement and admixture on autogenous shrinkage of cement paste”, Cement and Concrete Research, Vol.25, No.2:281-287.
11. ASTM C1698-09. Standard Test method for autogenous strain of cement paste and mortar. In: ASTM international, West Conshohocken (PA); 2010.

12. ASTM C596-09. Standard Test method for drying shrinkage of mortar containing hydraulic cement. In: ASTM international, West Conshohocken (PA); 2010.

CHAPTER 4. GENERAL CONCLUSIONS

General Discussion

The objectives of this study were (1) to find a new approach to describe the relationship between penetration and elapsed time and to predict concrete setting behavior by using the maturity concept, as well as (2) to develop a statistical model to describe and predict the shrinkage behavior of HPC containing SCMs and to evaluate the effects of SCMs on the shrinkage behavior of HPC. Based on the observations and conclusions presented in chapters 2 and 3, the main conclusions of this study are as follows:

1. The concrete maturity approach and exponential model ($\varepsilon_{auto/drying}(t) = a + b * e^{(c*t)}$) successfully described and predicted the concrete setting behavior and shrinkage of high-performance concrete with SCMs. In the former (the concrete maturity approach), the correct initial and final setting times indicated the appropriate times for surfacing, jointing, and formwork removal. In the latter (the exponential model), the statistical model provided a better understanding of shrinkage behavior in HPC by giving the physical meanings—such as ultimate shrinkage, shrinkage rate at an early age, and shrinkage rate at middle age—on which to model coefficients a, b, and c in the exponential model equation above. This equation can estimate the total shrinkage of high-performance concrete at any age up to 56 days.
2. Class C fly ash is a good SCM in high-performance concrete. The literature shows fly ash has a mixed effect on concrete setting time. Twenty percent fly

ash replacement increased initial concrete setting time by 15% and final concrete setting time by 10% at the temperatures of 65^{o}F, 75^{o}F, and 85^{o}F, which indicates fly ash provides a longer working time in concrete construction, such as when placing and filling formwork. This conclusion was also used to determine the final setting time of mortar for HPC with 20% fly ash replacement in study 2, thus significantly reducing the number of setting time tests. In addition, 30% fly ash replacement can reduce both autogenous shrinkage and free drying shrinkage by as much as 20% and, therefore, reduces the risk of shrinkage cracking.

3. Addition of GGBF slag increased the autogenous shrinkage; however, it also reduced the free drying shrinkage. Therefore, it had no significant overall effect on the total shrinkage.
4. Clear linear relationship was observed between autogenous shrinkage and free drying shrinkage at early concrete ages up to 14 days: free drying shrinkage = 6 x autogenous shrinkage + 176, no matter what kind of SCMs I used. With this equation, users can predict the shrinkage at an early age if one of these variables is known.

Recommendations for Future Research

The experimental works have provided comprehensive studies of the relationship between concrete setting behavior and maturity, and autogenous and free drying shrinkage in high-performance concrete. However, future research is still required,

especially for concrete datum temperature determination. As presented in chapter 2, a datum temperature of 4^{o}C was selected for the concrete maturity calculation. Although the literature supported this concrete maturity calculation, future experimental work is still needed. In order to improve the penetration resistance–maturity curve, A systemically designed study of the effects of chemical admixtures and SCMs on datum temperature is highly recommended.

In addition, the study results indicate the following:

1. To evaluate the maturity properties of high-performing concrete and to develop a similar statistical model for shrinkage, add more supplementary cementitious materials, such as silica fume, metakaolin, or Class F fly ash.
2. Researchers should do more experimental work on autogenous and free drying shrinkage of high-performance concrete mixtures to calibrate and access the validity of the model.
3. In the future, researchers should conduct more in-depth investigations on the effects of multiple variables (e.g., combination of SCMs, cement type, water-cement ratio, chemical admixtures, and ambient moisture and temperature) on autogenous and free drying shrinkage of HPC to achieve more definite conclusions.
4. Based on the literature review, slag effects on concrete setting behavior are controversial. Therefore, researchers should also conduct similar studies using slag replacements.

APPENDIX A

NOMENCATURE

HPC	high-performance concrete
NSC	Normal strength concrete
SCMs	supplementary cementitious materials
FA	fly ash
GGBFS	ground granulated blast-furnace slag
RS	relative shrinkage
RIS/RFS	relative initial/final set
AEA	air entraining agent
ASTM	American Society for Testing and Materials
ACI	American Concrete Institute

APPENDIX B

C-3WR MIXDESIGN WORK SHEET (STUDY 1)

PROJECT:		
PROJECT TITLE:	Work Time Limit for Retarders	
MIX TYPE:		
MIX NUMBER:	C-3WR	
W/C(+FLY ASH):	0.41	
CEMENT:		
Type	I	
Source	Lehigh	
Specific Gravity	3.14	
Volume Of Cement	0.108	(enter as ft3)
Total Cementitious Material	571	
FLY ASH:		
Class		
Source		
Specific Gravity		
% Substitution By Weight Of Cement	0.00	(enter 0 if none is used)
MINERAL ADMIXTURE:		
Class/Grade		
Source		
Specific Gravity		
% Substitution By Weight Of Cement	0.00	(enter 0 if none is used)
SILICA FUME SLURRY:		
Source		
Specific Gravity		(dry silica)
Specific Gravity		(slurry)
Specific Weight		(silica slurry, enter as lbs/gal)
Specific Weight		(water, enter as lbs/gal)
Specific Weight		(dry silica, enter as lbs/gal)
% Substitution By Weight Of Cementitiou	0.00	(dry silica, enter 0 if none used)
Slurry Water Contibution	0.0	(calculated lbs)
Dry Silica Added	0.0	(calculated lbs)
FINE AGGREGATE:		
Source	Cordova	
Specific Gravity	2.67	
% of Total Aggregate	45.00	
COARSE AGGREGATE:		
Source	Ft. Dodge	
Specific Gravity	2.66	
% of Coarse and Intermediate Aggregate	100.00	
% of Total Aggregate	55.00	(calculated)
INTERMEDIATE AGGREGATE:		
Source		
Specific Gravity		
% of Coarse and Intermediate Aggregate	0.00	(calculated)
% of Total Aggregate	0.00	(calculated)
AIR ENTRAINING AGENT:		
Brand	AEA 92, Euclid	
oz/100 lbs cementitious	0.8	(enter 0 if none is used)
RETARDER:		
Brand		
oz/100 lbs cementitious	0.0	(enter 0 if none is used)
WATER REDUCER:		
Brand	Daratard 18	
oz/100 lbs cementitious	3.5	(enter 0 if none is used)
SUPER WATER REDUCER:		
Brand		
oz/100 lbs cementitious	0.0	(enter 0 if none is used)
ACCELERATOR:		
Brand		
oz/100 lbs cementitious	0.0	(enter 0 if none is used)
SLUMP:		
Design	2.0	(enter as in)
AIR CONTENT:		
Design	6.0	(enter as %)
BATCH SIZE:	1.30	(enter as ft3)

GENERAL INFORMATION

PROJECT:	0
PROJECT TITLE:	Work Time Limit for Retarders
MIX TYPE:	0
MIX NUMBER:	C-3WR
DATE:	2/11/2011

MATERIALS	*Source*	*Type/Class*	*SPG*	*Percen*	*Percent*
CEMENT:	Lehigh	I	3.14		
FLY ASH:				0.00	
MINERAL ADMIXTURE:				0.00	
SILICA FUME SLURRY:				0.00	
FINE AGGREGATE:	Cordova		2.67	45.00	
COARSE AGGREGATE:	Ft. Dodge		2.66	55.00	100.00
INTERMEDIATE AGGREGATE:				0.00	0.00
AIR ENTRAINING AGENT:	AEA 92, Euclid				
RETARDER:					
WATER REDUCER:	Daratard 18				
SUPER WATER REDUCER:					
ACCELERATOR:					
DESIGN W/C(+FLY ASH):	0.41				
DESIGN SLUMP:	2.0				
DESIGN AIR CONTENT:	6.0				

QUANTITIES (absolute volume method in SSD condition)

	Volume ft3 Batch Size 1.0 yd3	Volume ft3 Batch Size 1.0 ft3						Weight lbs Batch Size 1.0 ft3	Weight lbs Batch Size 1.0 yd3	Weight lbs Lab Batch Size 1.30
CEMENT:	2.9160	0.1080	X	3.14	X	62.4	=	21.2	571	27.5
FLY ASH:	0.0000	0.0000						0.0	0	0.0
MINERAL ADMIXTURE:	0.0000	0.0000						0.0	0	0
SILICA FUME SLURRY:	0.0000	0.0000						0.0	0	0
WATER:	3.7541	0.1390	X	1.00	X	62.4	=	8.7	234	11.3
FINE AGGREGATE:	8.4195	0.3118	X	2.67	X	62.4	=	52.0	1403	67.5
COARSE AGGREGATE:	10.2905	0.3811	X	2.66	X	62.4	=	63.3	1708	82.2
INTERMEDIATE AGGREGATE:	0.0000	0.0000						0.0	0	0.0
AIR:	1.6200	0.0600	X	0.00	X	62.4	=	0.0	0	0.0
Summation	**27.0000**	**1.0000**						**145.1**	**3916**	**188.6**
Paste Content	**24.7**									
Mortar Content (abs vol)	**61.9**									
Mortar Content (% pass)	**30.7**									

CHEMICAL ADMIXTURES

	Rate oz/100 lbs cementitious							Rate ml Batch Size 1.0 ft3	Rate ml Batch Size 1.0 yd3	Rate ml Lab Batch Size 1.3
AIR ENTRAINING AGENT:	0.8	21.16	X	0.008	X	29.6	=	4.7	126.7	6.1
RETARDER:										
WATER REDUCER:	3.5	21.16	X	0.035	X	29.6	=	21.9	591.3	28.5
SUPER WATER REDUCER:										
ACCELERATOR:										

APPENDIX C

TYPICAL JMP REGRESSION DATA SHEET FOR AUTO 10% FA

Fit Curve
Model Comparison

Model	AICc	BIC	SSE	MSE	RMSE	R-Square
Exponential 3P	244.63629	249.19375	2407.0016	80.233386	8.9573091	0.9875103

Plot

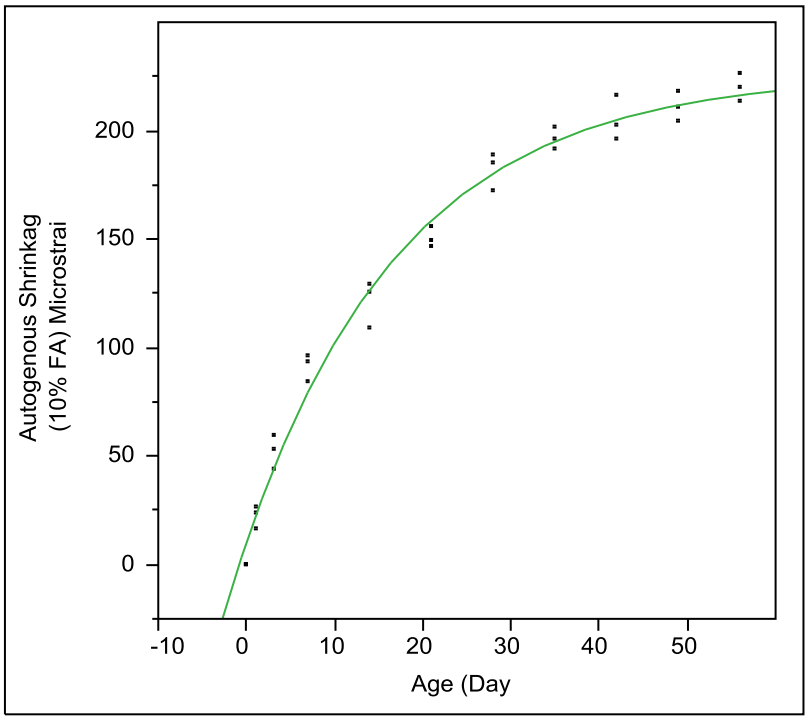

Exponential 3P
Prediction Model

a+b*Exp[c*Age (Day)]

a=Asymptote

b=Scale

c=Growth Rate

Summary of Fit

AICc	244.63629
BIC	249.19375
SSE	2407.0016
MSE	80.233386
RMSE	8.9573091
R-Square	0.9875103

Parameter Estimates

Parameter	Estimate	Std Error	Lower 95%	Upper 95%
Asymptote	225.96224	5.2689418	215.63531	236.28918
Scale	-215.7364	5.2702774	-226.0659	-205.4068
Growth Rate	-0.055572	0.0041387	-0.063684	-0.04746

Correlation of Estimates

	Asymptote	Scale	Growth Rate
Asymptote	1.0000	-0.7863	0.8819
Scale	-0.7863	1.0000	-0.5418
Growth Rate	0.8819	-0.5418	1.0000

Covariance of Estimates

	Asymptote	Scale	Growth Rate
Asymptote	27.7617	-21.834	0.0192
Scale	-21.834	27.7758	-0.0118
Growth Rate	0.0192	-0.0118	0.0000

APPENDIX C

TOTAL SHRINKAGE PREDICTED VS ACTUAL JMP REGRESSION SHEET

Bivariate Fit of Predicted Shrinkage (Microstrain) By Actual Shrinkage (Microstrain)

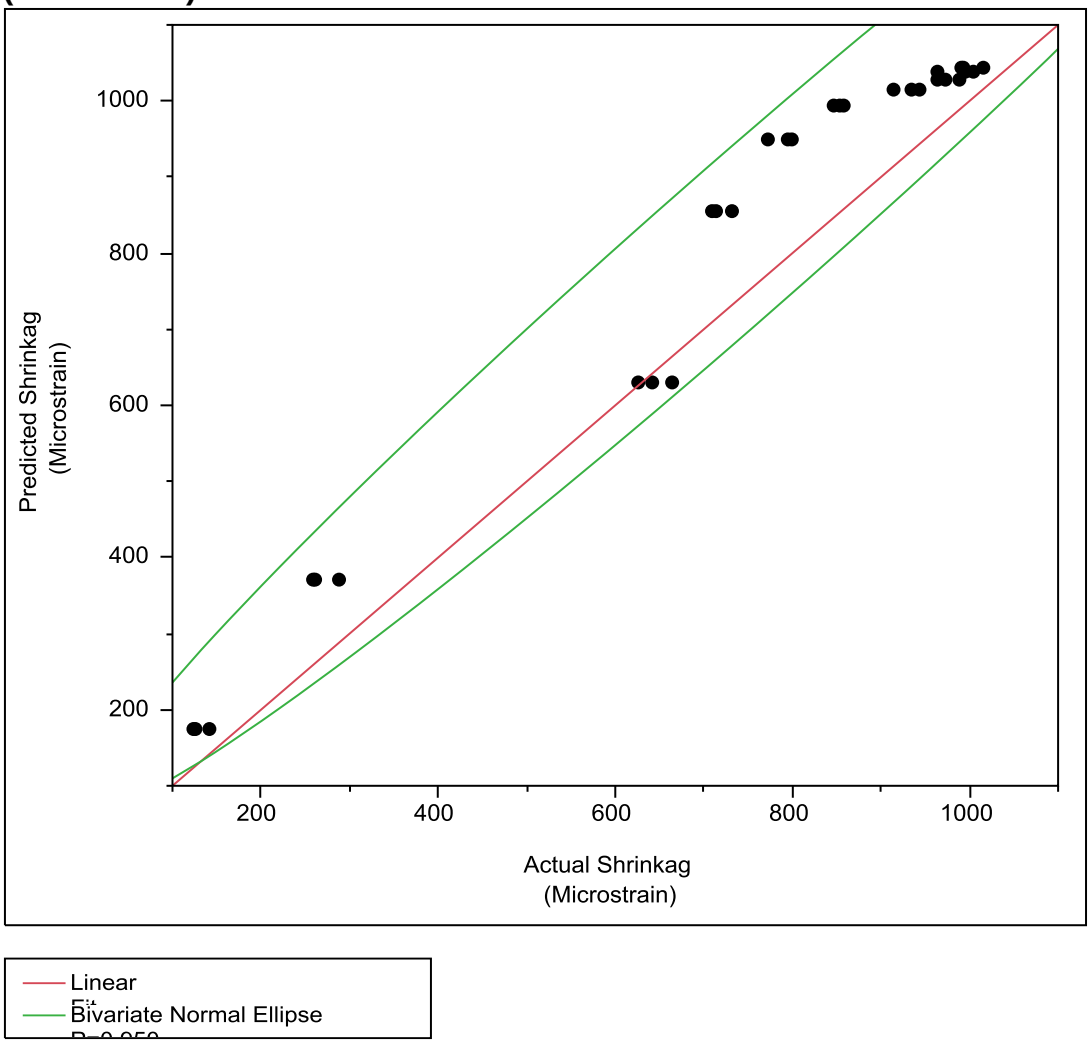

Linear Fit

Predicted Shrinkage (Microstrain) = 0 + 1*Actual Shrinkage (Microstrain)

Summary of Fit

RSquare	.
RSquare Adj	.
Root Mean Square Error	94.03671
Mean of Response	808.6
Observations (or Sum Wgts)	30

Analysis of Variance

Source	DF	Sum of Squares	Mean Square	F Ratio
Model	0	.	0.00	.
Error	30	265287.11	8842.90	**Prob > F**
C. Total	30	.		.

Tested against reduced model: Y=0

Parameter Estimates

Term		Estimate	Std Error	t Ratio	Prob>|t|
Intercept	Constrained	0	0	.	.
Actual Shrinkage (Microstrain)	Constrained	1	0	.	.

APPENDIX D

SHRINKAGE DATA

Auto (Microstrain)							
Age (Day)	25% GGBFS	35% GGBFS	45% GGBFS	PC	10 % FA	20 % FA	30% FA
0	0	0	0	0	0	0	0
1	30	31	34	28	22	18	14
3	55	74	89	61	52	46	42
7	103	116	127	106	91	86	72
14	147	164	181	134	121	107	88
21	172	198	223	158	147	132	111
28	197	229	262	188	179	152	139
35	229	254	294	208	196	177	153
42	251	277	307	233	202	184	153
49	259	286	323	242	208	192	161
56	264	292	332	246	222	202	167

Drying (Microstrain)							
Age (Day)	25% GGBFS	35% GGBFS	45% GGBFS	PC	10 % FA	20 % FA	30% FA
0	0	0	0	0	0	0	0
1	264	347	350	287	312	276	294
3	588	566	621	544	491	455	504
7	777	823	864	733	742	696	731
14	987	942	958	988	938	847	829
21	1023	1044	1025	1087	1061	959	909
28	1055	1050	1030	1151	1090	980	920
35	1070	1050	1040	1168	1110	1000	930
42	1097	1054	1035	1180	1124	1008	941
49	1100	1055	1039	1187	1127	1009	944
56	1109	1057	1042	1194	1129	1011	945

Total (Microstrain)							
Age (Day)	25% GGBFS	35% GGBFS	45% GGBFS	PC	10 % FA	20 % FA	30% FA
0	0	0	0	0	0	0	0
1	294	378	384	315	334	294	308
3	643	640	710	605	543	501	546
7	880	939	991	839	833	782	803
14	1134	1106	1139	1122	1059	954	917
21	1195	1242	1248	1245	1208	1091	1020
28	1252	1279	1292	1339	1269	1132	1059
35	1299	1304	1334	1376	1306	1177	1083
42	1348	1331	1342	1413	1326	1192	1094
49	1359	1341	1362	1429	1335	1201	1105
56	1373	1349	1374	1440	1351	1213	1112